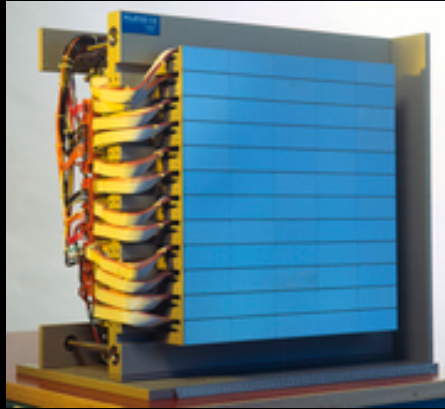
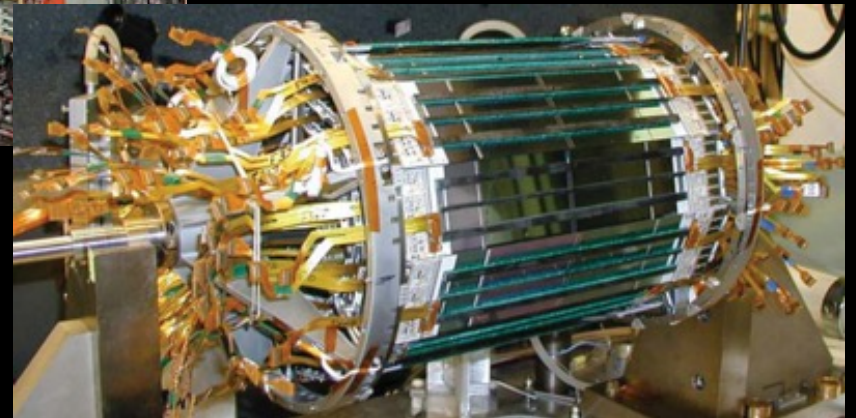
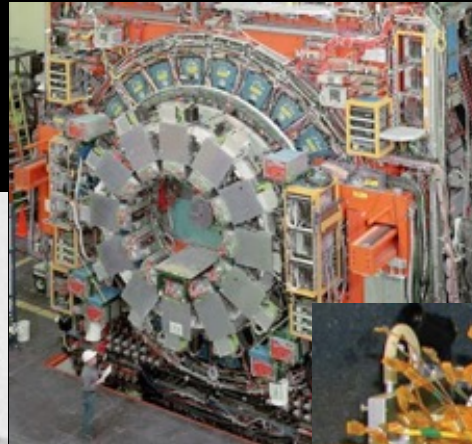
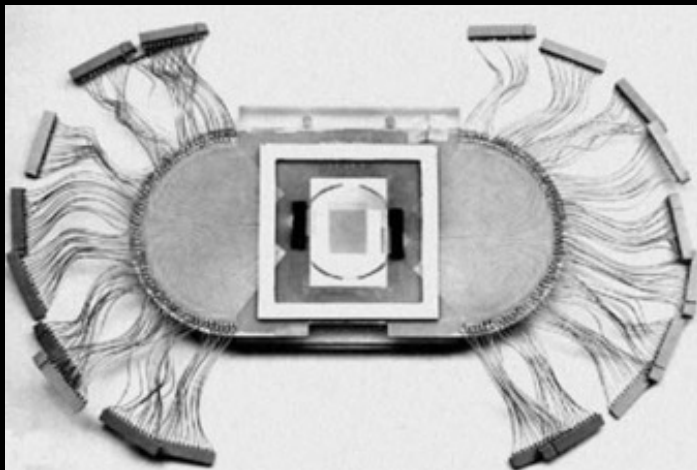
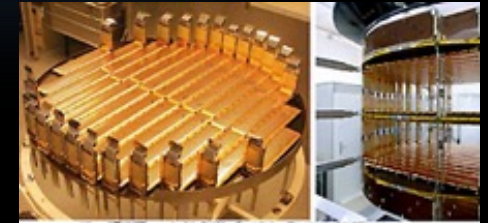


Silicon Detectors and Applications

Cinzia Da Via, Uni. Manchester IEEE NPSS Workshop on Applications of Radiation Instrumentation, 2020



Cinzia Da Vià
The University of Manchester, UK
Stony Brook University USA



Some Information about myself

- Professor at The University of Manchester (UK)
- Visiting Professor at the University of Stony Brook, New York, USA
- Member of the ATLAS Collaboration at CERN – LHC
- Spent 11 years at CERN during the LHC detector development working on radiation hard pixel detectors

Work Highlights:

- Detector development : scintillating fibers, silicon pixels
- Radiation effects in silicon, low temperature effects (Lazarus)
- 3D sensors for high energy physics and other applications
- 3D printed detectors
- Vertical integrated microsystems
- Quantum Imaging



This lecture

- Introduction on Radiation Interaction with Matter
- Why Silicon as a radiation detector
- Silicon radiation detectors: Strip and Pixel sensors Monolithic and Hybrid
- Novel silicon technologies: micro-fabricated 3D sensors, LGADS and microsystems (time permitting)
- Examples of applications in High Energy Physics, Medicine, Environmental Monitoring, Space..

Introduction: Imaging radiation ..



Web cams



Smart phones



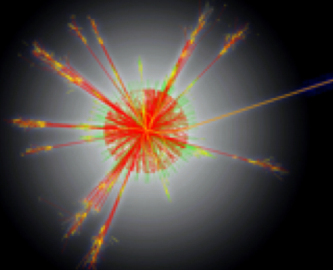
photo cameras



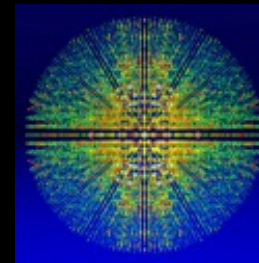
machine vision, automotive, security etc...



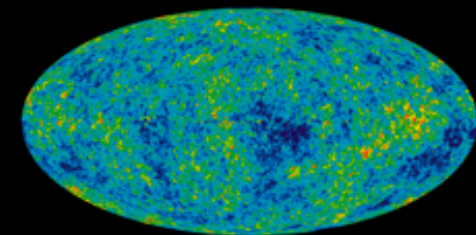
Medical imaging



HEP



x-ray crystallography

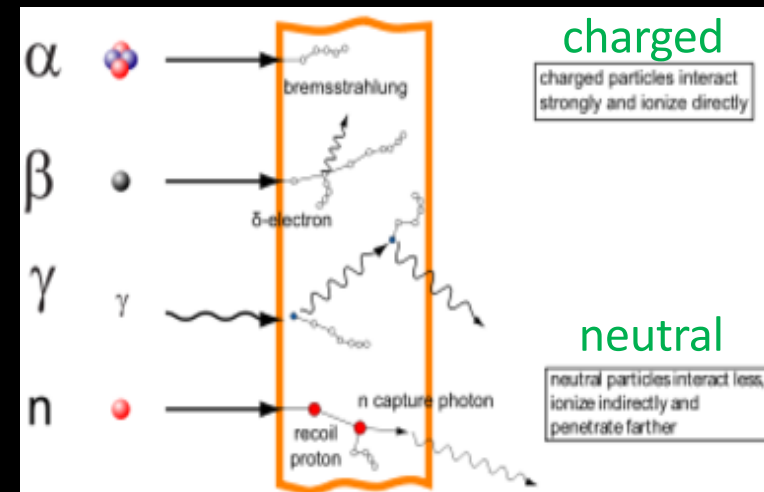
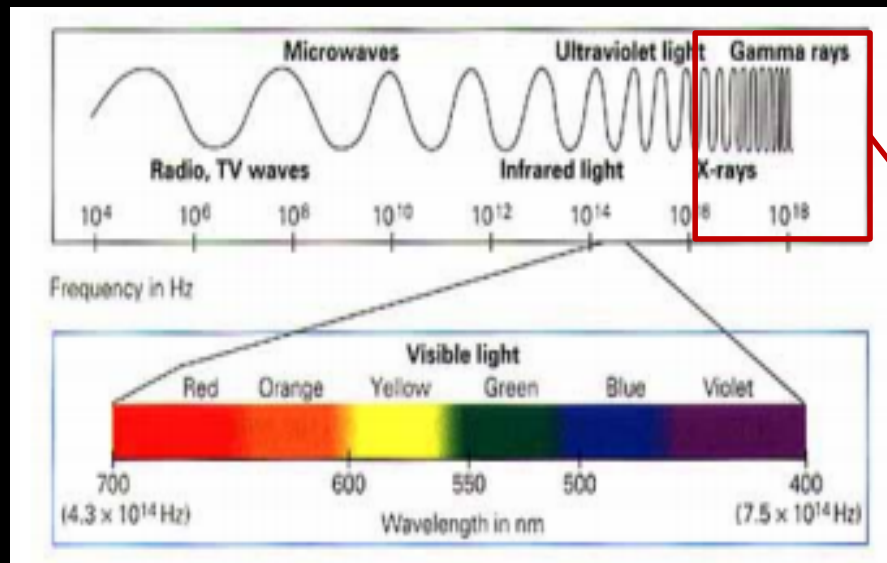


cosmology

mass spectroscopy, neutrons, electrons, TOF, SEM/TEM etc...

Reminder: What is Radiation and its interaction with matter

Radiation can be defined as the propagation of energy through space or matter in the form of electromagnetic waves or energetic particles.



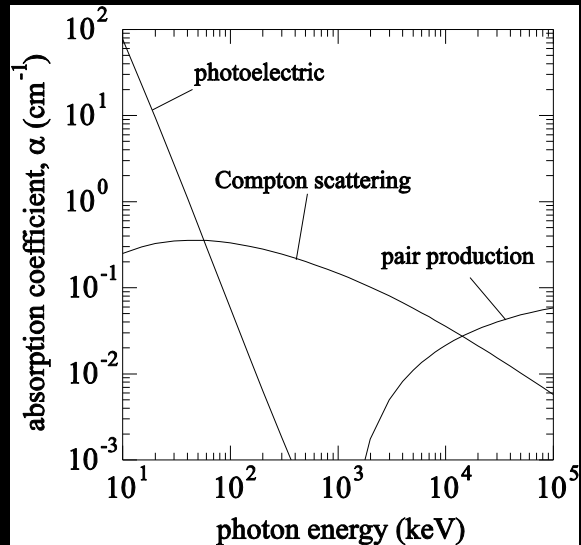
When radiation interacts with matter:

Non-ionizing does not have enough energy to ionize atoms but **generate heat** in the material it interacts with. At high energy it becomes ionizing

Ionizing has the ability to knock an electron from an atom, i.e. to ionize..

Interaction of radiation with matter

Cinzia Da Via, Uni. Manchester IEEE NPSS Workshop on Applications of Radiation Instrumentation, 2020



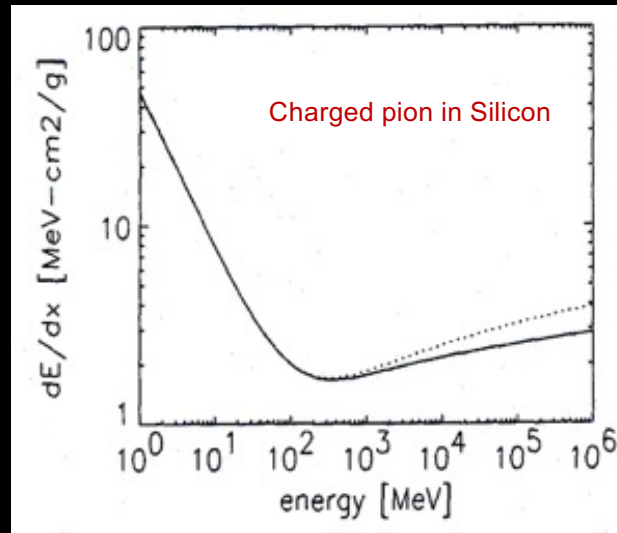
Photons:

There are 3 main modes of interaction:

- Photoelectric absorption
- Electron scattering
- Pair production

Lambert-Beer's law

$$\phi(x) = \phi_0 \cdot e^{-\alpha x}$$



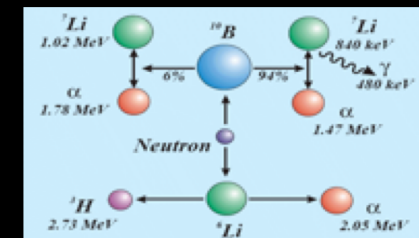
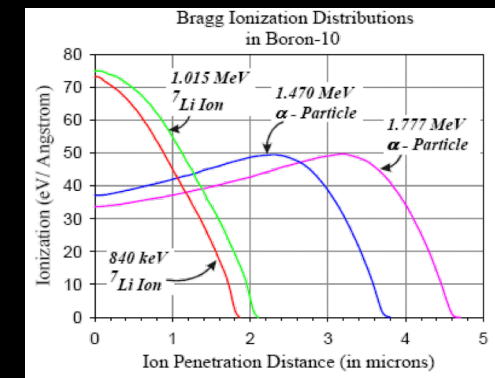
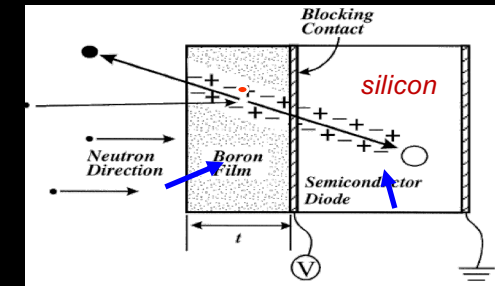
Ionizing particles:

Bethe-Bloch equation:

average/mean amount of energy lost due to ionization per unit of distance in the media)

$$-\frac{dE}{dx} = \frac{4\pi}{m_e c^2} \cdot \frac{n z^2}{\beta^2} \cdot \left(\frac{e^2}{4\pi\epsilon_0}\right)^2 \cdot \left[\ln\left(\frac{2m_e c^2 \beta^2}{I \cdot (1 - \beta^2)}\right) - \beta^2 \right]$$

$$n = \frac{N_A \cdot Z \cdot \rho}{A \cdot M_u}$$

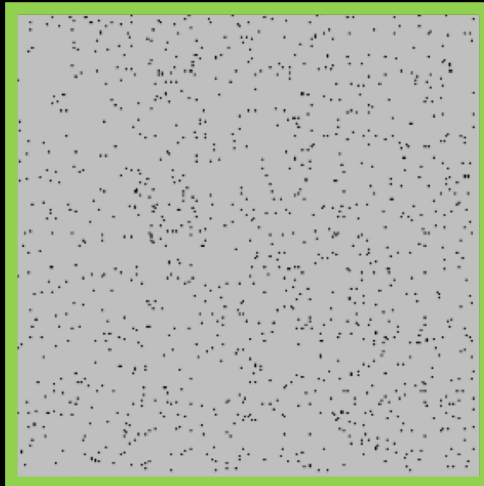


Neutrons: Alpha Bragg peak

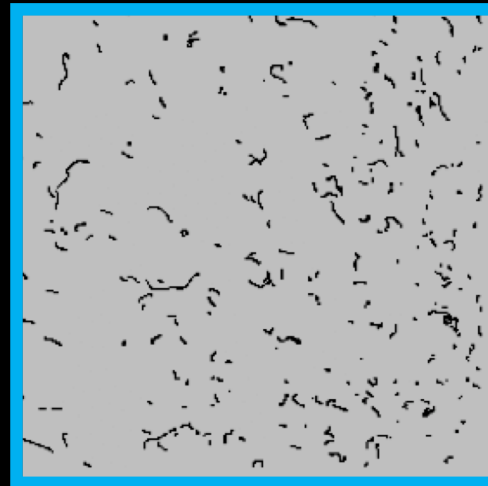
Particle signatures with the Timepix detector

→ See next talk on Timepix detectors

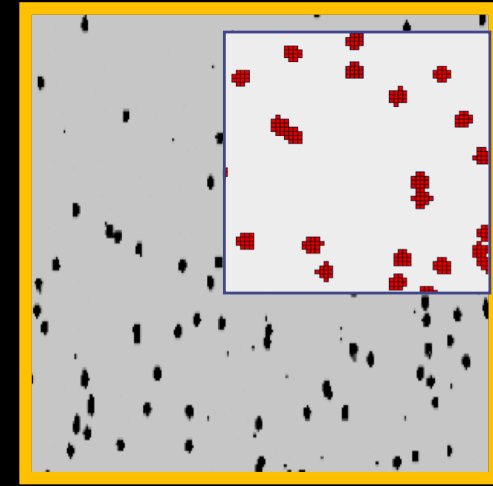
5 KeV X-rays



2MeV electrons



α



- ◆ ^{241}Am alpha source gives clusters of $\sim 5 \times 5$ pixels measured with the MEDIPIX-USB device and a $300 \mu\text{m}$ thick silicon sensor. The clusters are shown in detail in the inset. The cluster sizes depend on particle energy and threshold setting.
- ◆ Signature of X-rays from a ^{55}Fe X-ray source. Photons yield single pixel hits or hits on 2 adjacent pixels due to charge sharing.
- ◆ A ^{90}Sr beta source produces curved tracks in the silicon detector.
- ◆ A pixel counter is used just to say “YES” if individual quantum of radiation generates in the pixel a charge above the pre-selected threshold

The semiconductors revolution

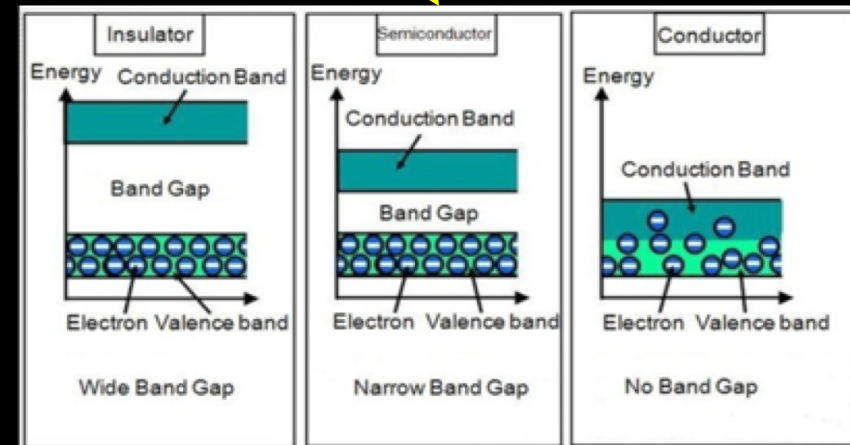
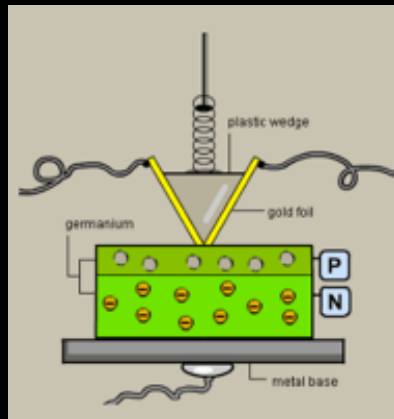
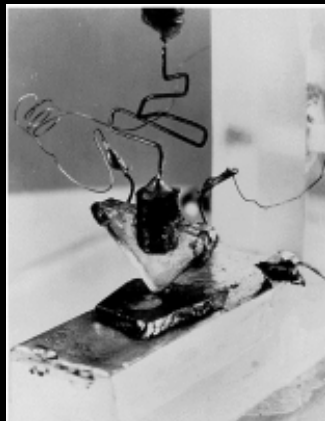


First transistor invented 1947 by William B. Shockley, John Bardeen and Walter Brattain (Nobel Prize 1956)



First semiconductor particle sensor: Pieter Jacobus Van Heerden, *The Crystalcounter: A New Instrument in Nuclear Physics*. University Math Naturwiss, Fak (1945). *CCD Nobel prize Boyle & Smith 2009*

A **Semiconductor** is a material that has a conductivity between a conductor and an insulator; electricity can pass through it, but not very easily



The point contact germanium transistor

Why Silicon is still the most used

- ❖ Semiconductor with Low ionization energy → big signal
The band gap is 1.12 eV, but it takes 3.6 eV to ionize an atom. The remaining energy goes to phonon excitations (heat)
- ❖ High purity → long carrier lifetime
- ❖ High mobility → fast charge collection
- ❖ Low Z → Z=14 low multiple scattering but low x-ray detection efficiency
- ❖ Oxide (SiO₂) has excellent electrical properties
- Good mechanical properties → Easily patterned to small dimensions
- Can be operated in air and at room temperature (before irradiation – afterwards requires cooling)
- Industrial experience and commercial applications
- **Silicon is abundant! Over 90% of the Earth's crust is composed of silicate minerals**
making silicon the second most abundant element in the Earth's crust (about 28% by mass) after oxygen

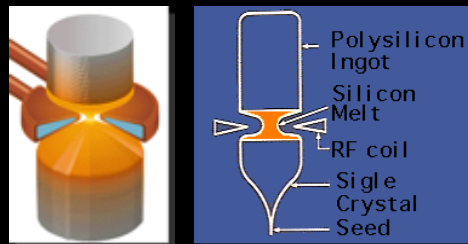
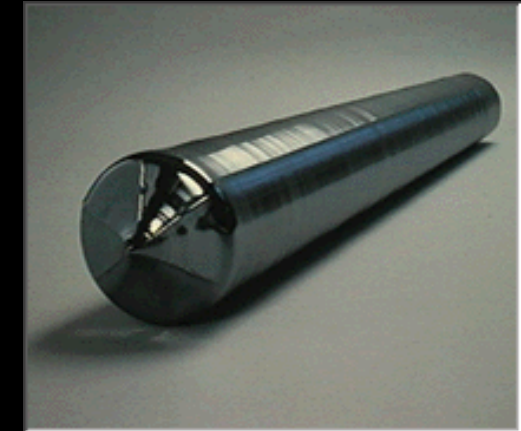
Parameter	cBN	hBN	Diamond	AlN	GaN	3C-SiC	GaAs	Si
Energy Bandgap (eV)	6.4	5.2	5.45	6.2	3.39	3.00	1.43	1.12
Electron Mobility (cm ² /Vs)	280	-	2200	300	440	400	8500	1500
Hole Mobility (cm ² /Vs)	-	-	1600	30	~20	50	400	600
Thermal Conductivity (W/cm K)	13	a = 6.0 c = 0.3	20	2.9	1.3	5	0.46	1.5
Breakdown (× 10 ⁵ Vcm ⁻¹)	~80	~80	100	~80	~80	40	60	3
Lattice Constant (Å)	3.615	a = 2.504 c = 6.661	3.567	4.982	a = 3.189 c = 5.185	4.358	5.65	5.43
Thermal Expansion Coefficient (× 10 ⁻⁶ °C ⁻¹)	3.5	a = -2.7 c = 38	1.1	4.0	4.5	4.7	5.9	2.6
Density (gm/cm ³)	3.487	2.28	3.515	3.26	6.15	3.216	5.316	2.328
Melting Point (°C)	2973	3000	3800	2200	>2500	2540	1238	1420
Dielectric Constant	7.1	5.1	5.5	-	9.5	9.7	12.5	11.8
Resistivity (Ωcm)	10 ¹⁶	10 ¹⁰	10 ¹³	10 ¹⁴	10 ¹²	150	10 ⁸	10 ³
Absorption Edge (µm)	0.205	0.212	0.20	-	0.35	0.40	-	1.40
Refractive Index	2.17	1.80	2.42	2.00	2.33	2.65	3.4	3.5
Hardness (kg/mm ² , T = 300 K Kg/mm ²)	5000	100	10,000	2500	1100	3000	600	1000

SILICON: from sand to wafer

Cinzia Da Via, Uni. Manchester IEEE NPSS Workshop on Applications of Radiation Instrumentation, 2020

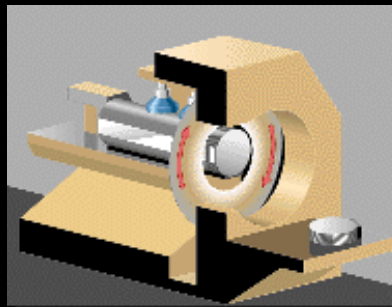


a) The sand is cleaned and further purified by chemical processes. It is then melted. Then a tiny concentration of phosphorus (boron) dopant is added to make n (p) type poly-crystalline ingots

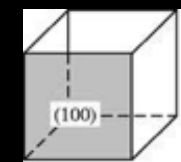
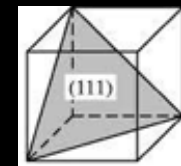


b) Single-crystal silicon is obtained by melting the vertically oriented poly-silicon cylinder onto a single crystal "seed" --- called "Float Zone-→ FZ"

c) Wafers of thickness 200- 500μm are cut with diamond encrusted wire or disc saws.

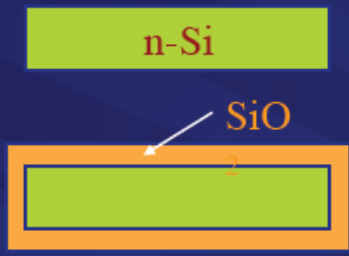



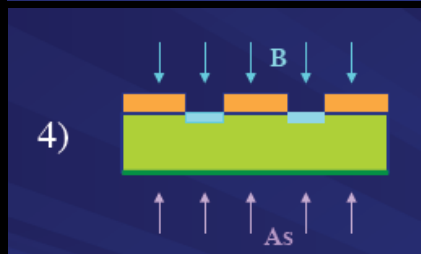
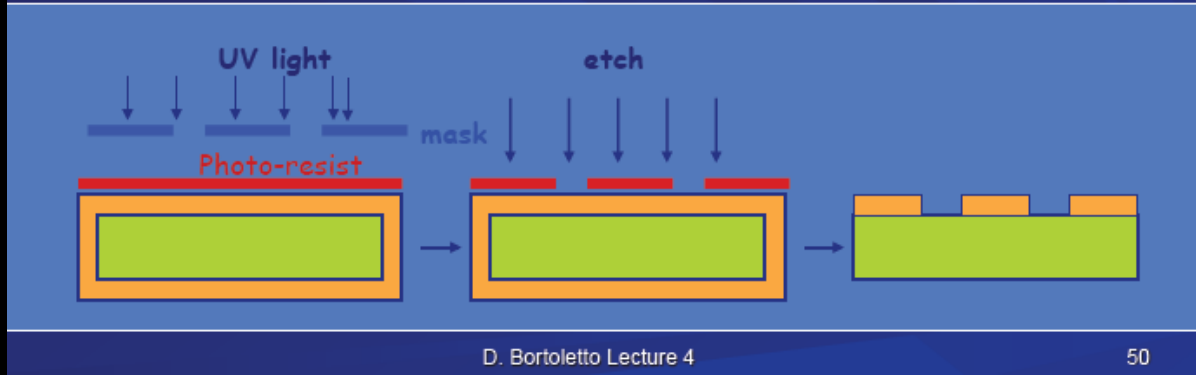
Note: the crystal orientation matters!
<111> and <100> crystals can influence the detector properties eg. capacitance



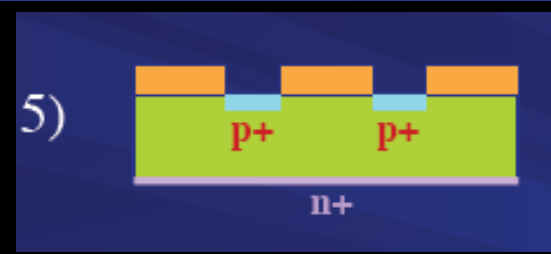
From Wafers to Sensors

Cinzia Da Via, Uni. Manchester IEEE NPSS Workshop on Applications of Radiation Instrumentation, 2020

- 1)  Start with n-doped silicon wafer, $\rho \approx 1-10 \text{ k}\Omega\text{cm}$. Silicon can be turned into n-type by neutron doping ($^{30}\text{Si} + n \rightarrow ^{31}\text{Si}$, $^{31}\text{Si} \rightarrow ^{31}\text{P} + \beta^- + \nu$)
- 2)  Oxidation at 800 - 1200°C
- 3) Photolithography (= mask align + photo-resist layer + developing) followed by etching to make windows in oxide



Doping (ion implantation or diffusion)



Crystal lattice annealing at 600C

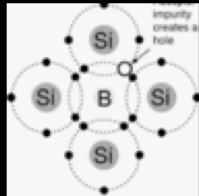
Note:

This process is used for single and double side processing



Photo-lithography
Followed by Aluminum
Deposition in the contact
Regions (front and back)

p-n Junction

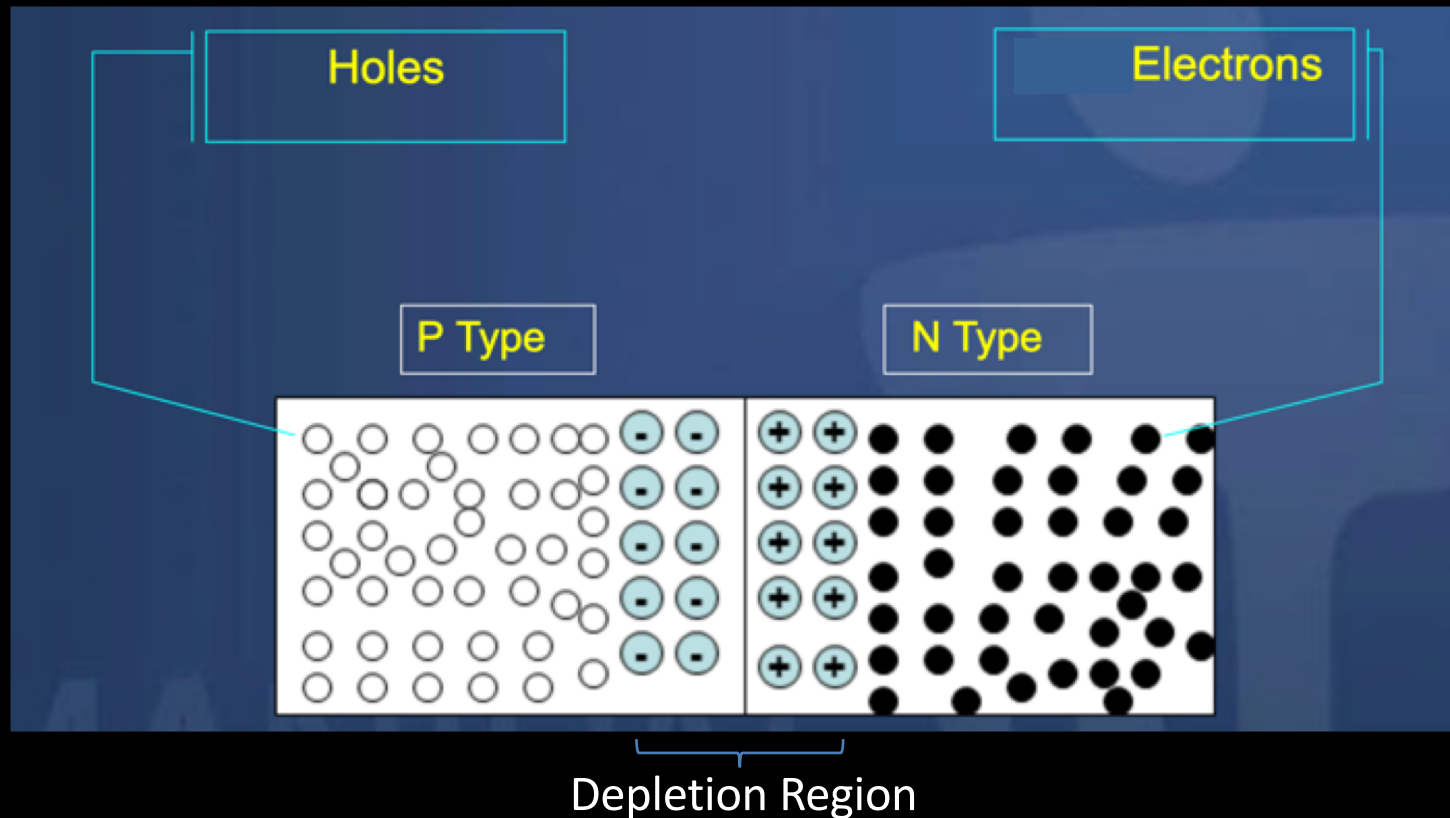
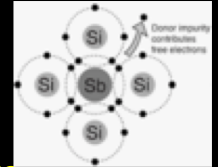


Doping: p-type Silicon

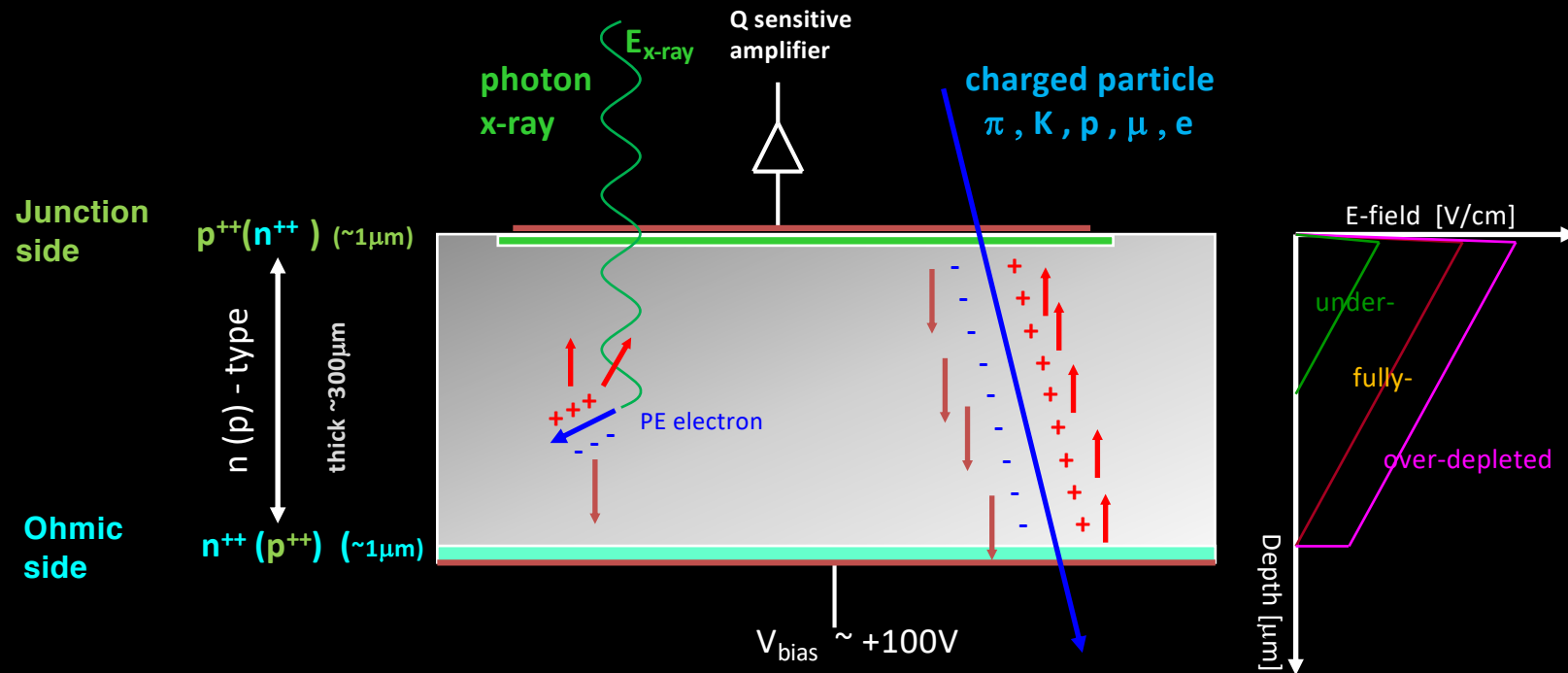
add elements from IIIrd group
 ⇒ acceptors (B,..)
 holes are majority carriers

Doping: n-type Silicon

add elements from Vth group
 ⇒ donors (P, As,..)
 electrons are majority carriers



Silicon detector basic working principle

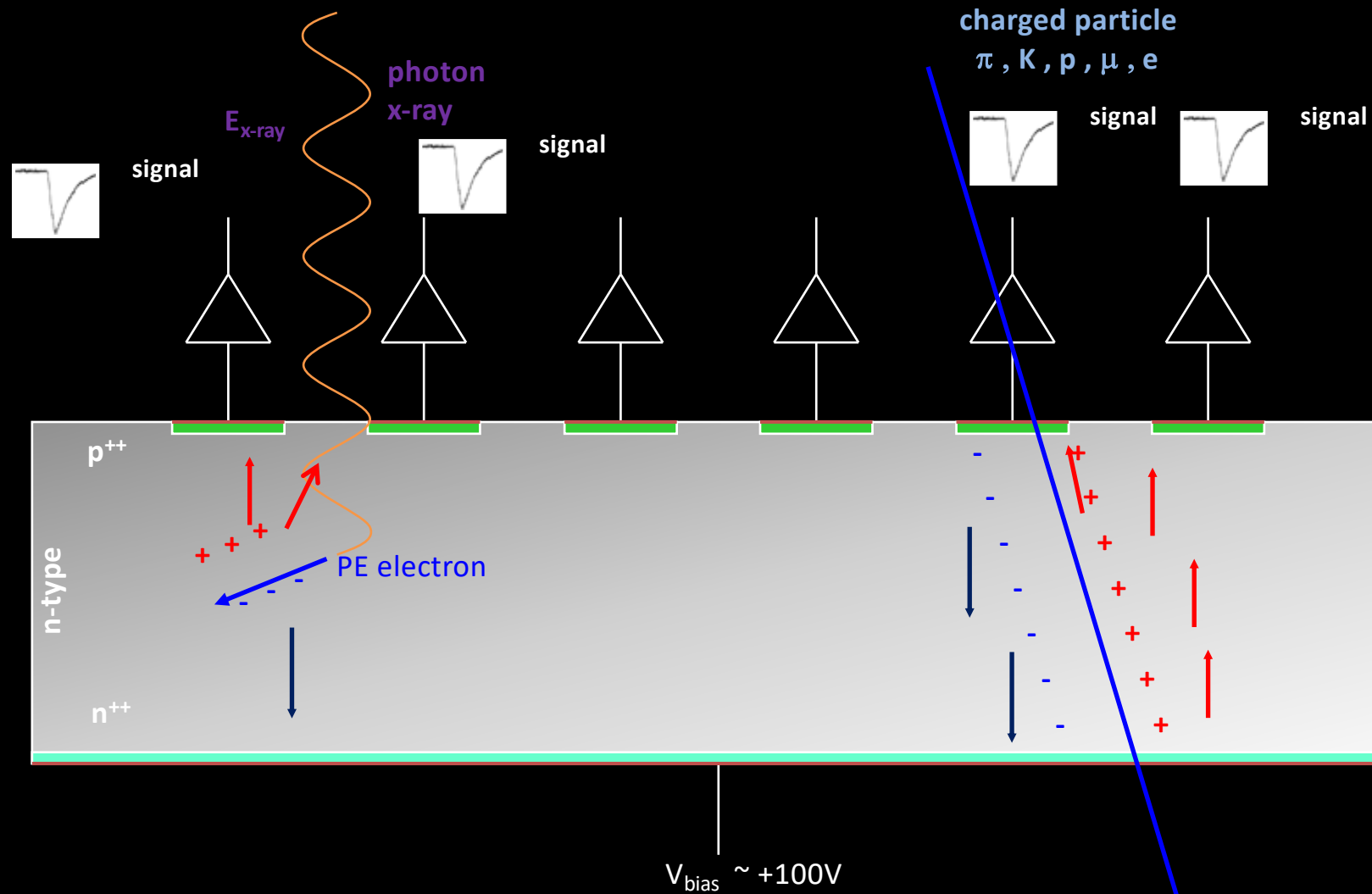


- ❖ n⁺ and p⁺ electrodes are implanted on the wafer's surfaces to form a p-i-n junction
- ❖ V_{bias} is the applied reverse bias voltage, W is the depletion region and N_{eff} the space charge (also called effective doping concentration)
- ❖ e-h pairs are created by the energy released by the impinging particle (different interaction mechanism for photons/x-rays and charged particles)
- ❖ e-h drift towards the positive and negative electrode "inducing" a current pulse
- ❖ Charge collection time depends on the carrier mobility, bias voltage and carrier polarity

$$V_{\text{bias}} = \frac{(W)^2 \times e \times |N_{\text{eff}}|}{2\epsilon_0 \epsilon_{\text{Si}}}$$

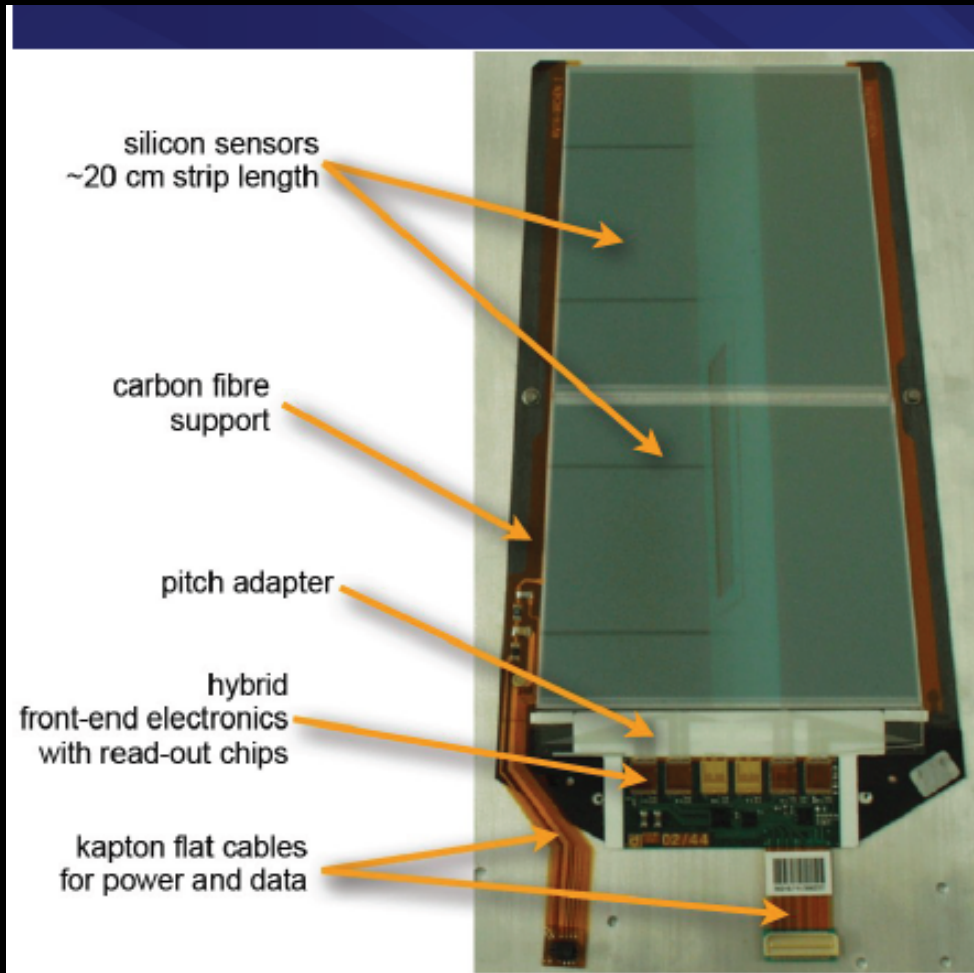
Segmented Silicon Sensors for better Position Sensitivity

Cinzia Da Via, Uni. Manchester IEEE NPSS Workshop on Applications of Radiation Instrumentation, 2020

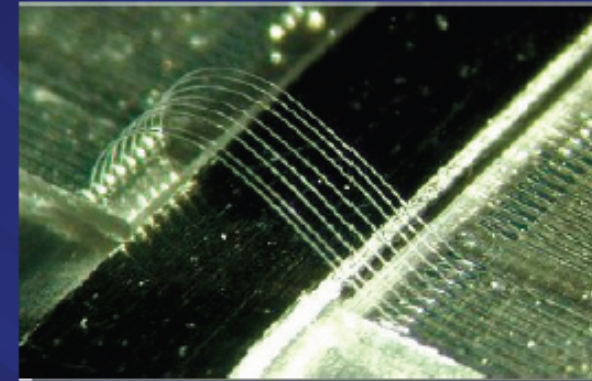


Example: CMS micro-strip module

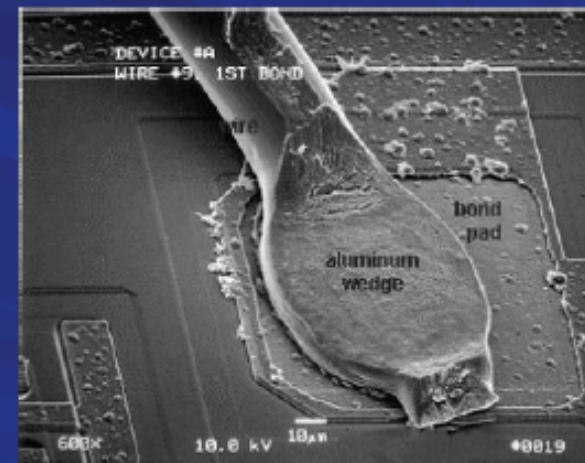
Cinzia Da Via, Uni. Manchester IEEE NPSS Workshop on Applications of Radiation Instrumentation, 2020



CMS strip module

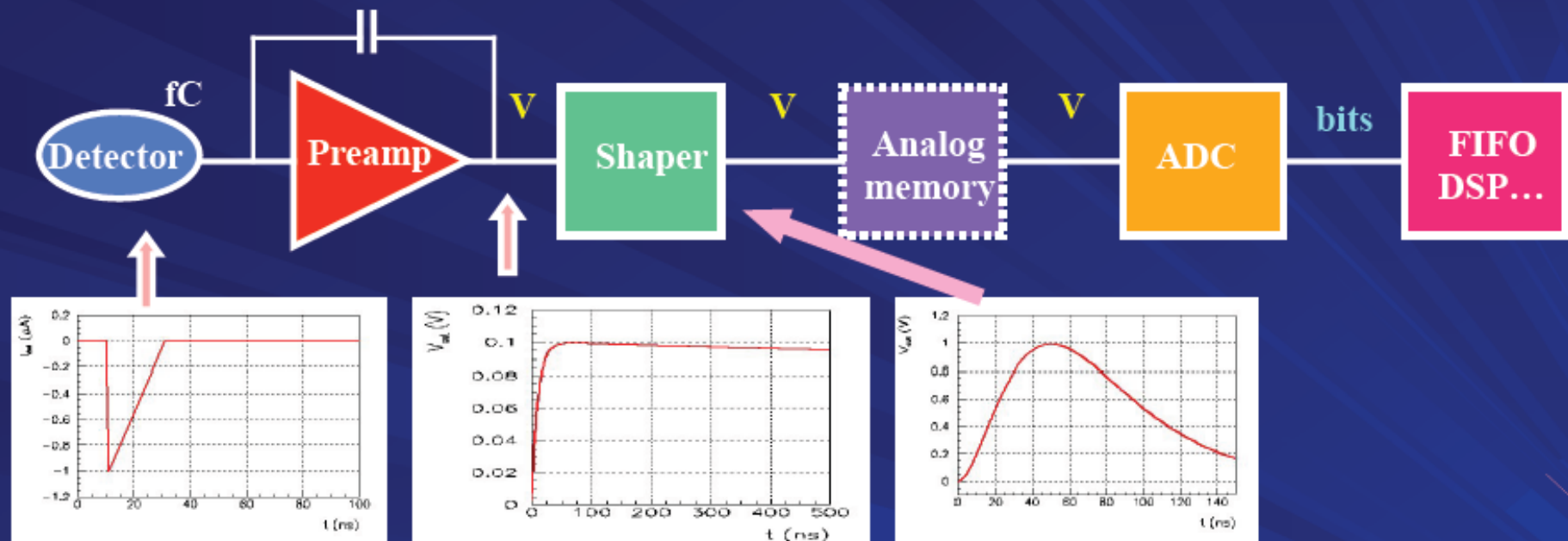


Wire-bonding



31

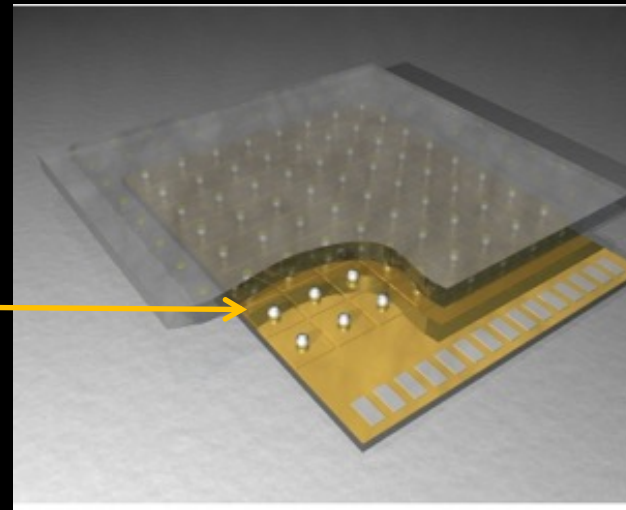
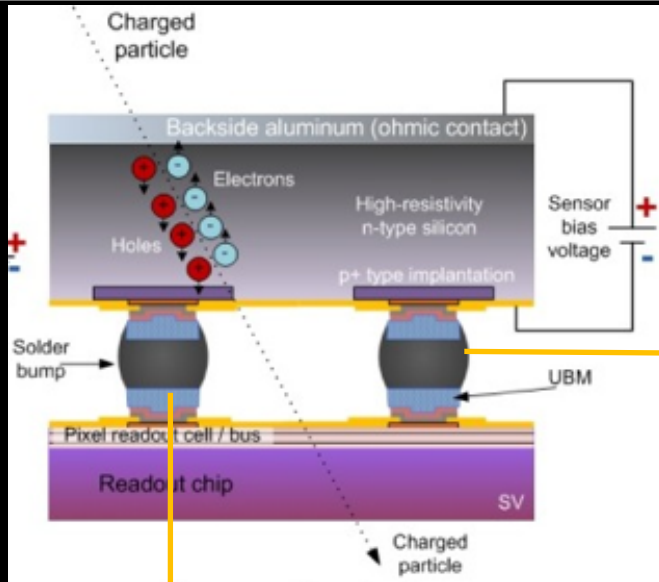
Front-end Readout electronics chain



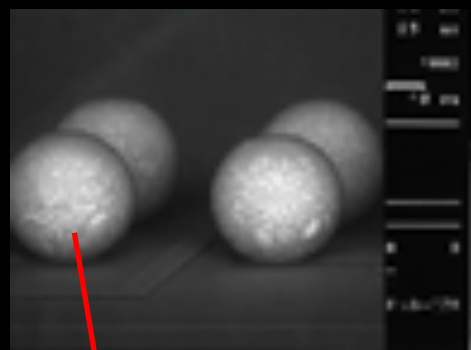
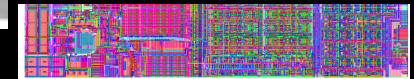
- Very small signals (fC) -> need **amplification**
- Measurement of **amplitude** and/or **time**
 - **(ADCs, discris, TDCs)** (Example Time over Threshold)
- Several thousands to millions of channels

Pixel Detectors "Hybrid"

Cinzia Da Via, Uni. Manchester IEEE NPSS Workshop on Applications of Radiation Instrumentation, 2020

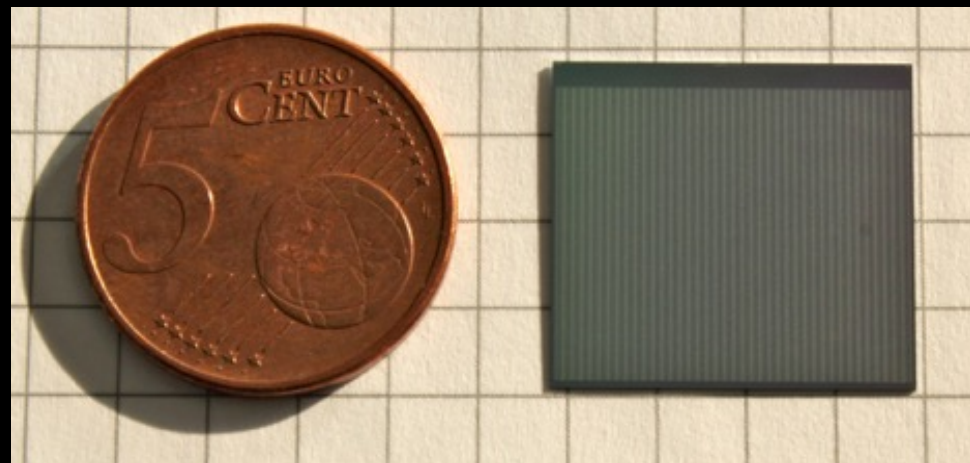


ATLAS FE-I4
80x336
=26 880 pixels
250 x 50 μm^2



50 microns

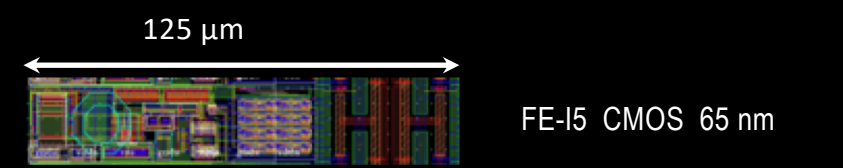
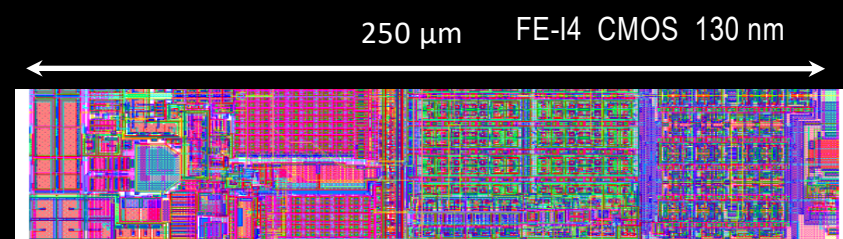
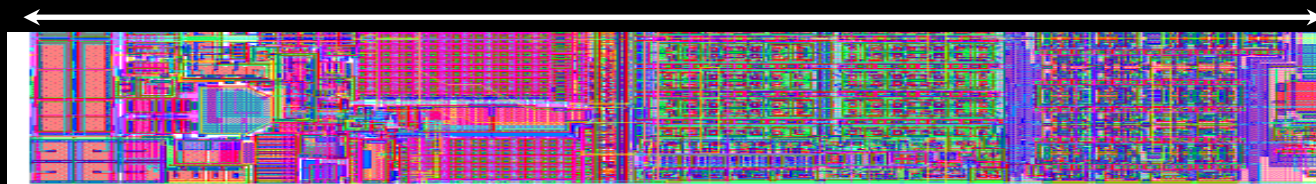
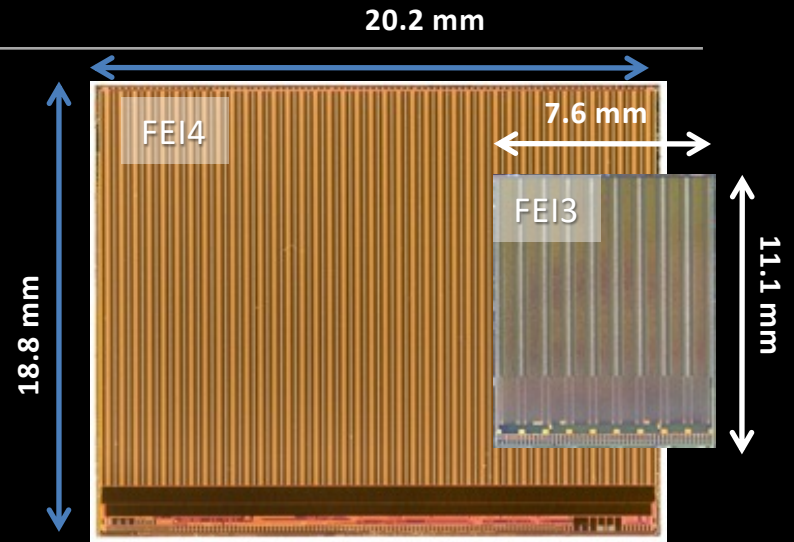
solder



ATLAS FE-I4 ~4cm²

Example: the ATLAS Pixel "FE-I" Family

	FEI4B	FEI3
Year	2011	2003
Technology	130nm	250nm
Chip size	20x19mm ²	7.6x10.8mm ²
Active area	89%	74%
Array	80x336 (26'880)	18x160 (2'880)
Pixel size	50x250μm ²	50x400μm ²
Number of transistors	87M	3.5M
Data rate	320 Mb/s	40Mb/s
Wafer yield	60%	80%



Half pitch definition

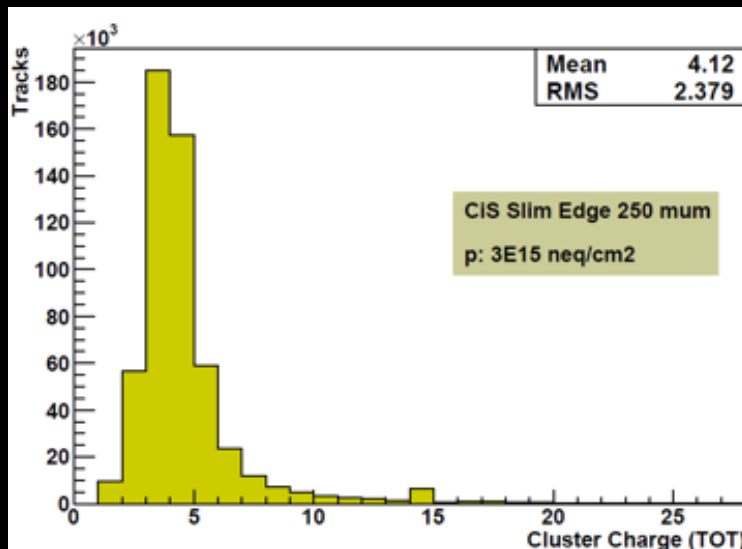
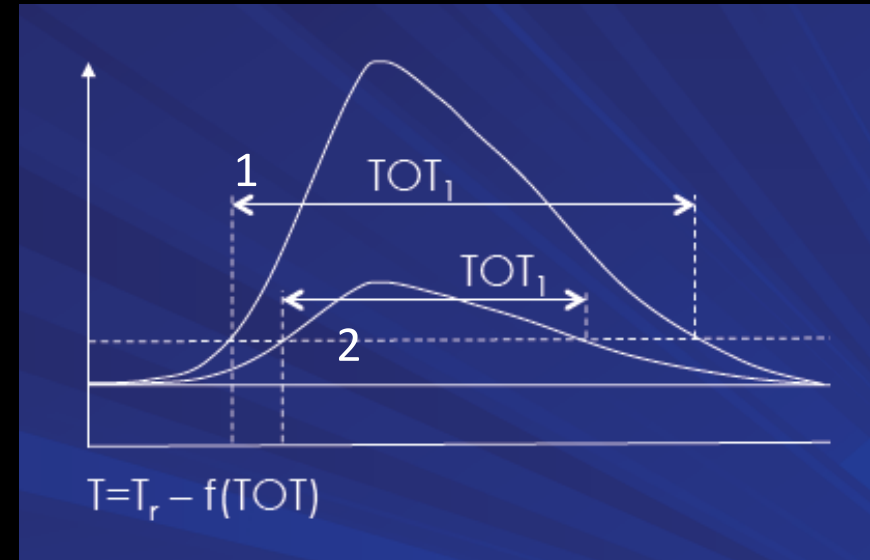
Depends on IC designs

250nm-130nm-65nm Technology nodes

DRAM MPU/ASIC 18

Time Over Threshold Electronics

- ❖ 1 TDC (Time to Digital Converter) channel measuring both leading edge and pulse width
- ❖ Single threshold timing: as soon as the signal is above threshold a digital signal is generated



- ❖ There is a dependence of the signal rise-time (1 and 2) and amplitude (“time walk”) which depends on the sensor capacitance C
- ❖ can even be used as an ADC (Analog to Digital Converter)
 - E.g. ATLAS Pixel

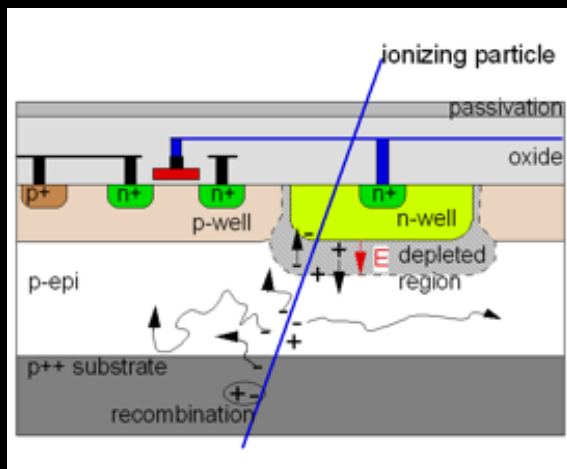
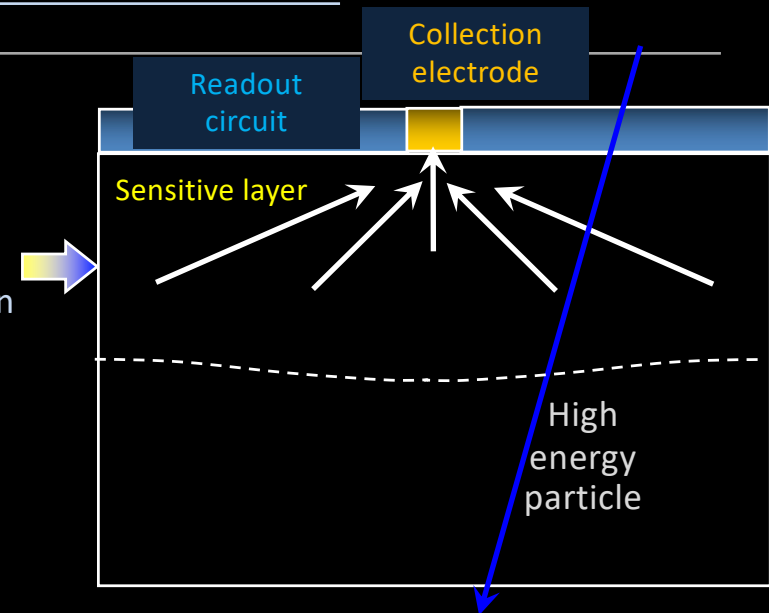
Pixel detectors “Monolithic”

Integrates the readout circuitry together with the detector in ‘one piece’ of silicon

The charge generated by a particle is collected on a defined collection electrode either by diffusion or by the application of an E-field

Small pixel size and thin effective detection thickness

Radiation soft, optimal for high granularity applications



IEEE TNS Vol: 56, Issue: 3, 2009

MAPS

Pixel size :
20 x 20 micron
Thickness
20-50 um

Used in the
EUDET telescope
And at STAR
At RICH

CCD

Charge
coupled
Device
Various
dimensions

Many uses in
Different
fields

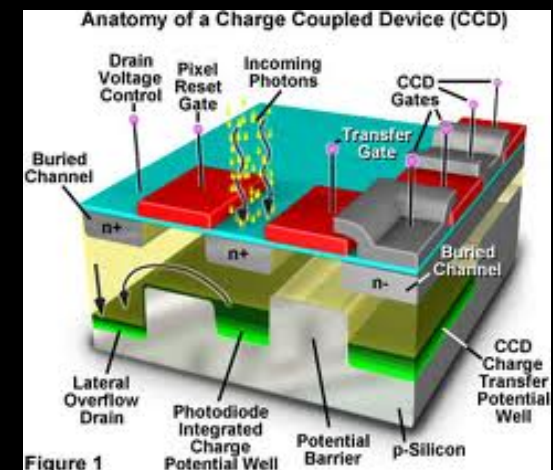


Figure 1

Pixels detectors and application requirements

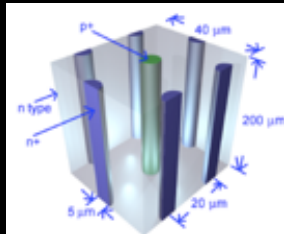
Hybrid

Monolithic

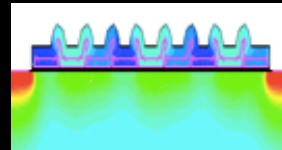
Radiation Hardness

Granularity, low mass

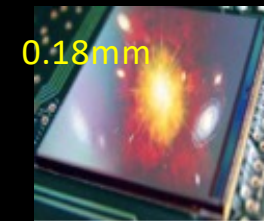
3D sensors



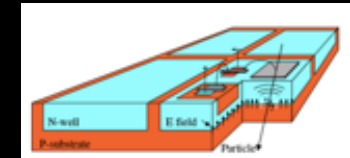
CCD



Mimosa



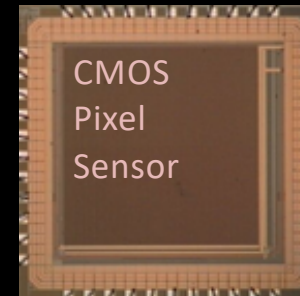
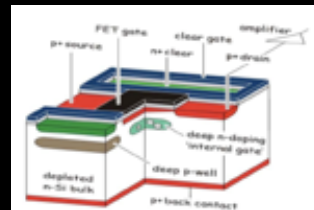
HV-MAPS



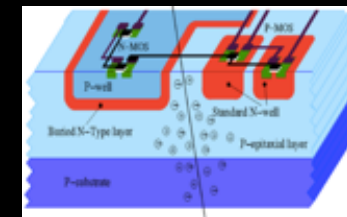
diamond



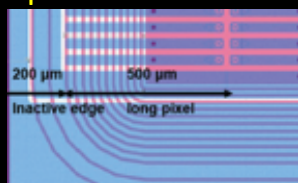
DEPFET



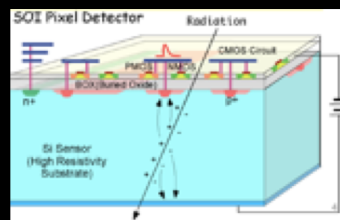
deepNwell



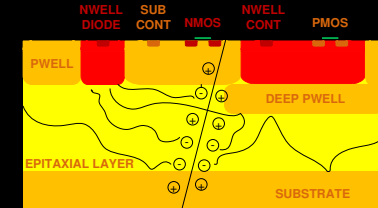
n-in-n, n-in-p-
planar



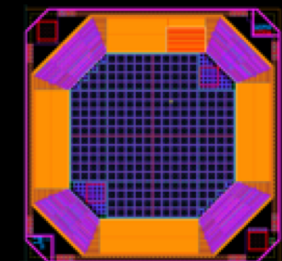
SOI



INMAPS

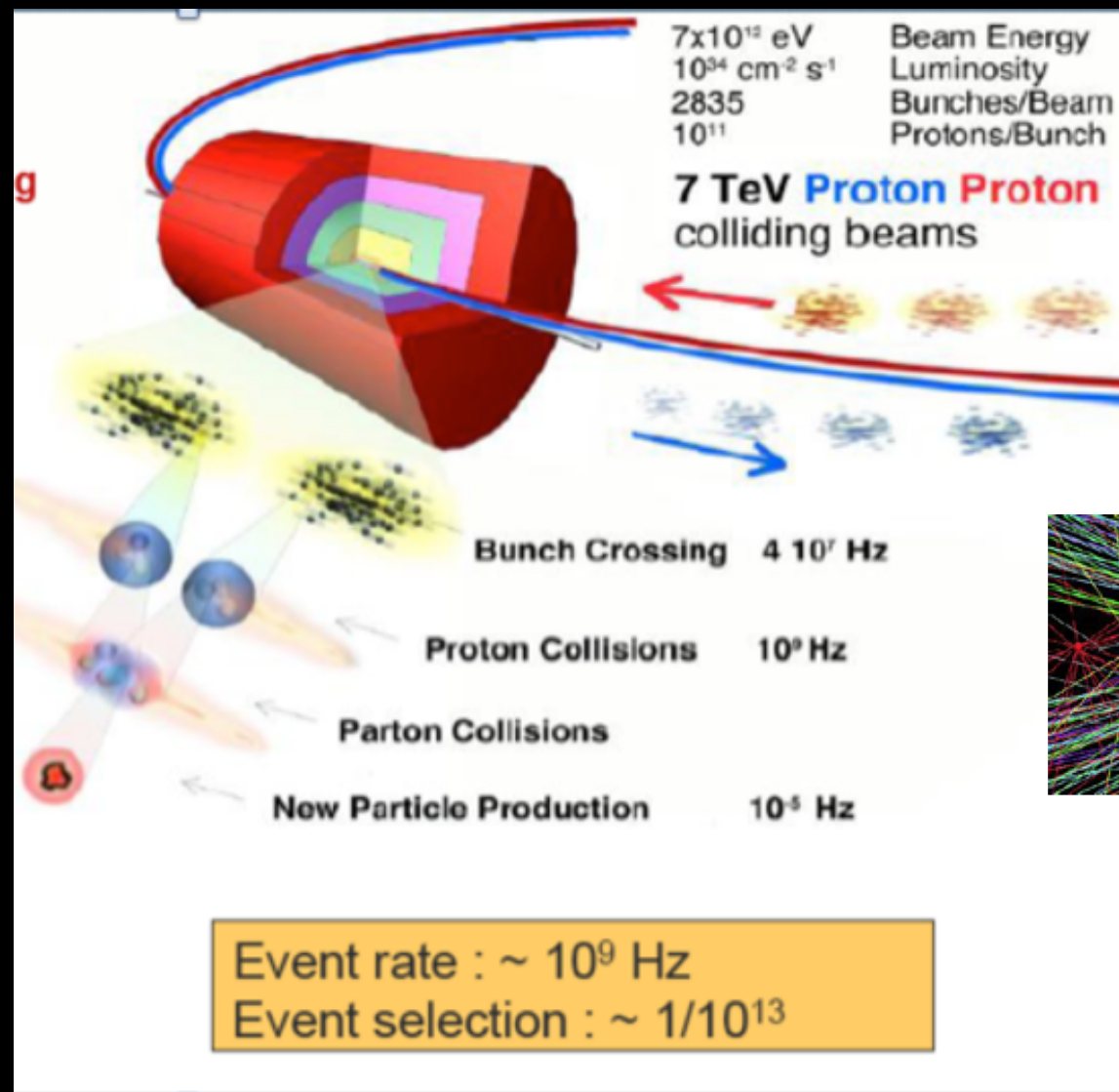


LePiX



The CERN Large Hadron Collider (LHC)

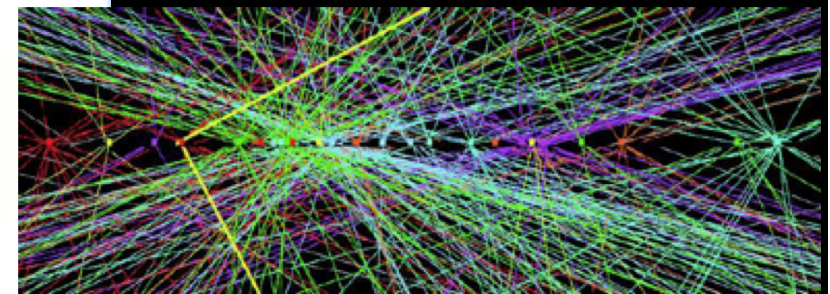
Cinzia Da Via, Uni. Manchester IEEE NPSS Workshop on Applications of Radiation Instrumentation, 2020



**A microscope to observe
Dimensions as small as
 10^{-17} m!**



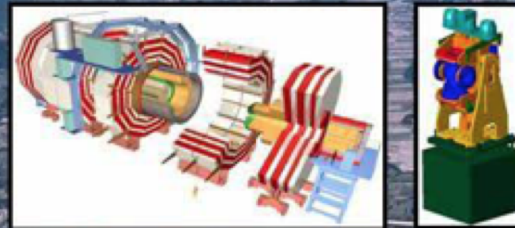
**Collisions
every 25 ns**



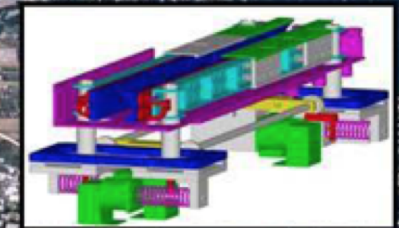
*Z -> $\mu\mu$ event
at LHC ATLAS
15 April 2012*

CERN-LHC
27 Km tunnel
~100m underground

CMS



LHCf



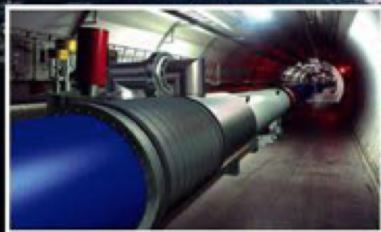
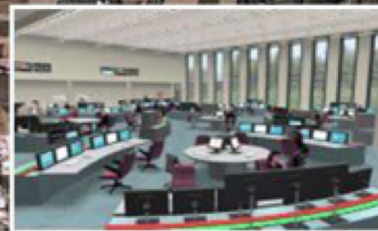
LHCb



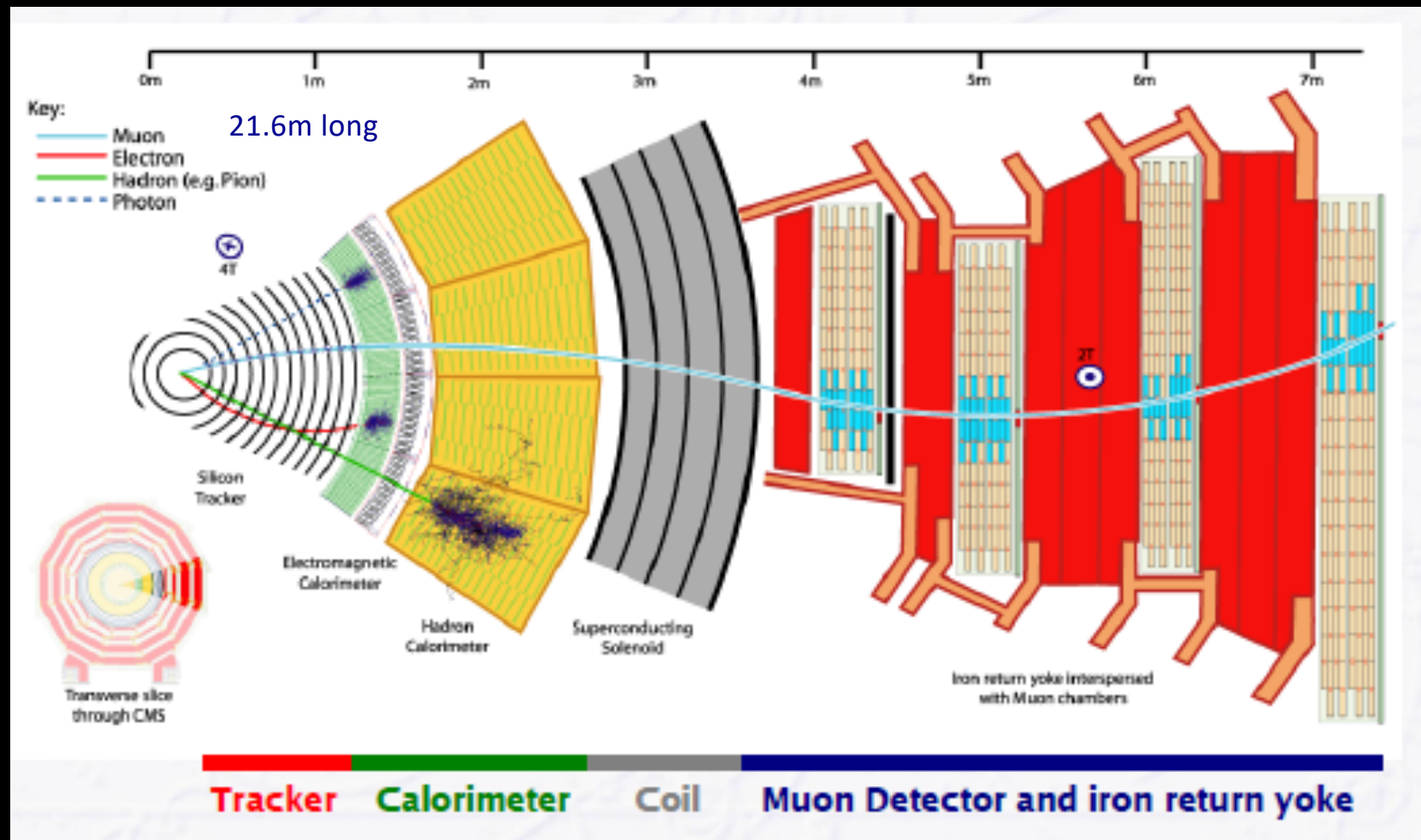
ATLAS



ALICE



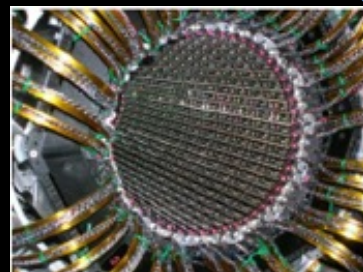
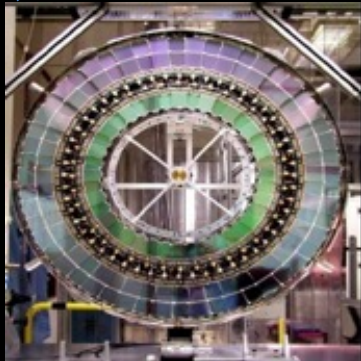
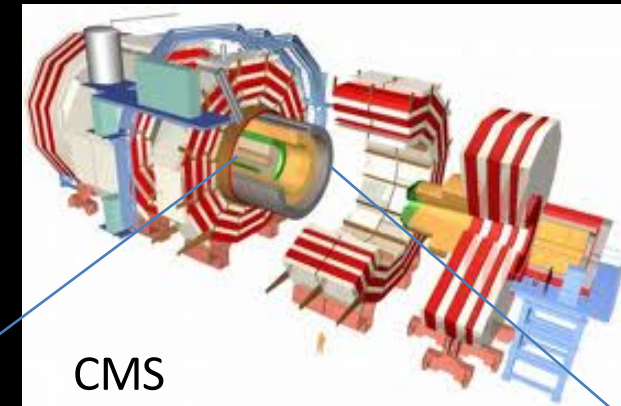
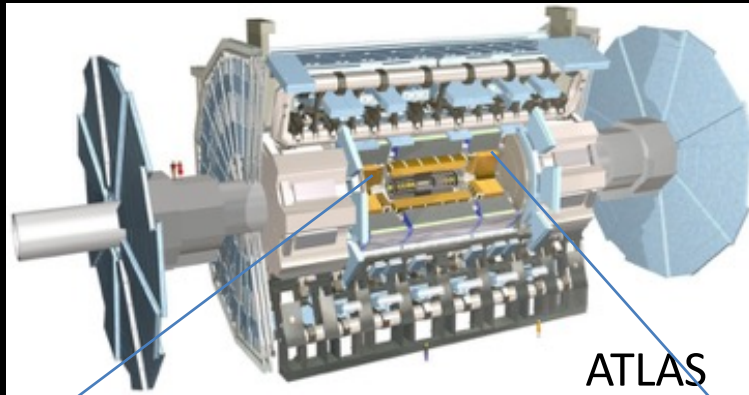
A typical particle detector: CMS



Silicon in the LHC Detectors



ATLAS and CMS use alone more than 250m² of Silicon Strips to “image” charged particles



Strips
61m² of silicon.
6.2million channels 4 barrel
layers + 9 disks per endcap
30cm < R < 52cm

Pixels
3 Barrel layers
(r=5,9,12 cm)
2 end caps each with
3 disks
80Mpixels
50x400um²
Digital I/O

Pixels
3 barrel layers
2 end caps each
with 2 disks
66 Mpixels 150 x 100um²
Analog I/O

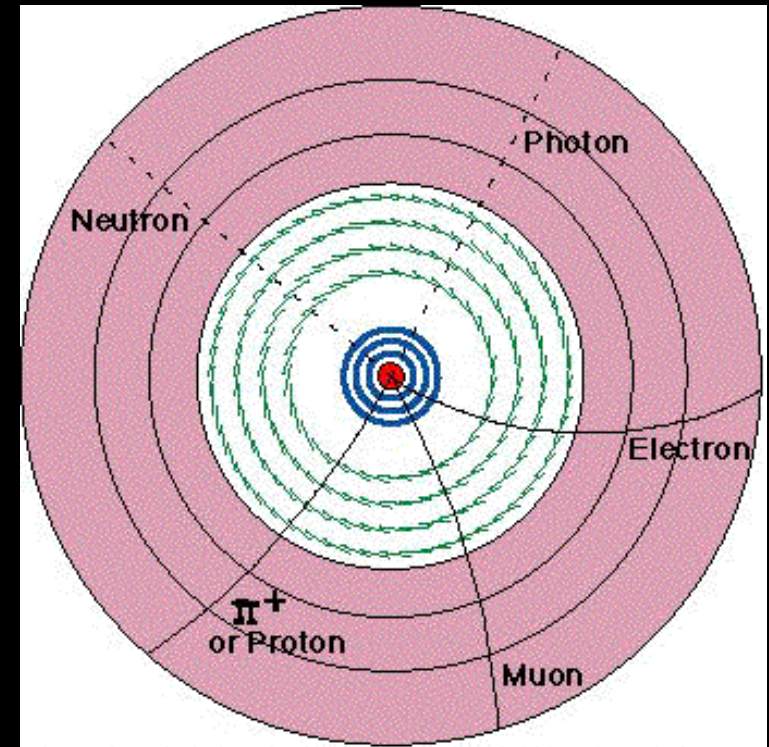
Strips
198 m² of silicon,
9.3 million channels
Inner : 4 barrel layers,
3 end-cap disks
Outer: 6 barrel layers,
9 weels
22cm < R < 120cm

Application1: Tracking Detectors

- Separate tracks by charge and momentum
- Position measurement layer by layer:

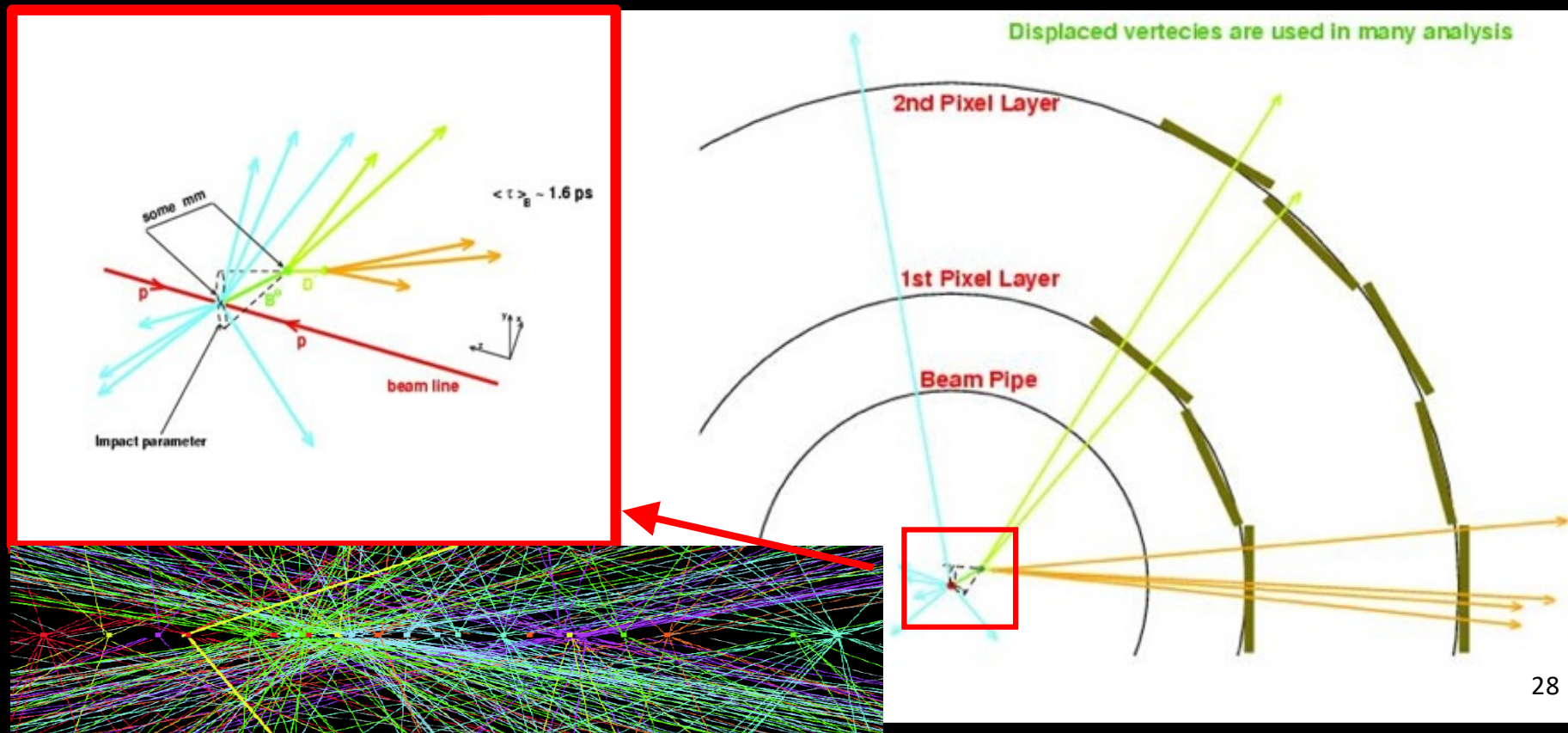
Inner layers: silicon
pixel and strips →
presence of hit
determines position

Outer layers: strips or “straw”
drift chambers → need
time of hit to determine
position



Example: Identification of Event Vertices

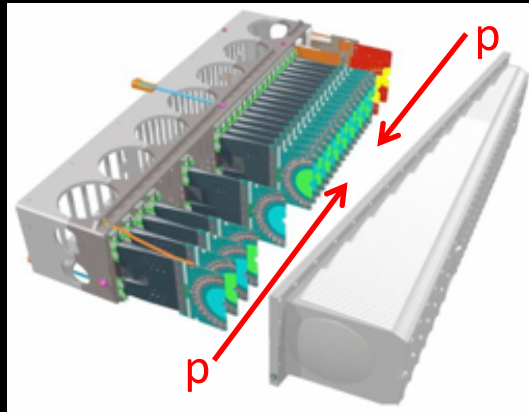
- primary event vertex reconstruction crucial in multiple collision events
- secondary vertices for live time tagging
- b- jet tagging



LHCb VERtex LOcator (VELO)

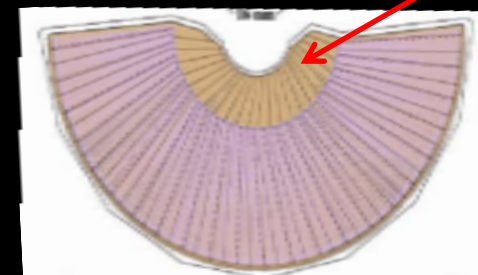
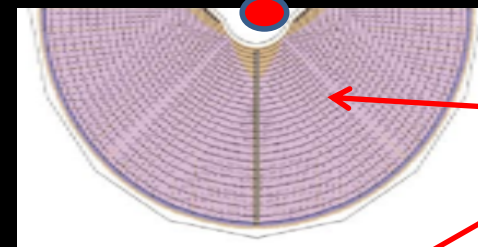
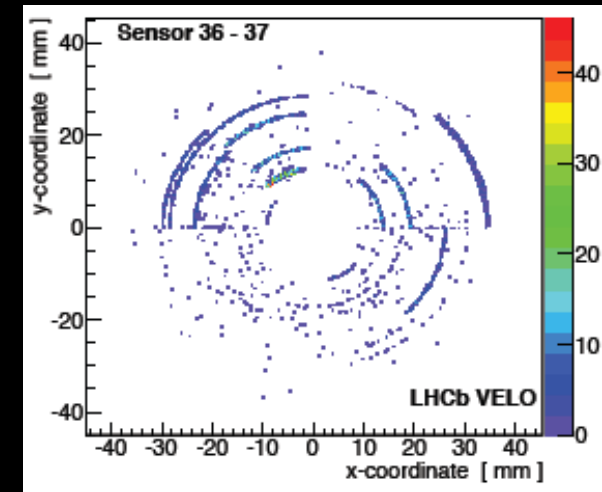
Search for physics beyond the Standard Model: CP-violation and rare decays of heavy hadrons

C. Farinelli



VELO characteristics:

- silicon sensors in secondary vacuum
- shielded by 300 μm RF foil
- 172,032 channels in total
- operating temperature of cooling system = -8°C

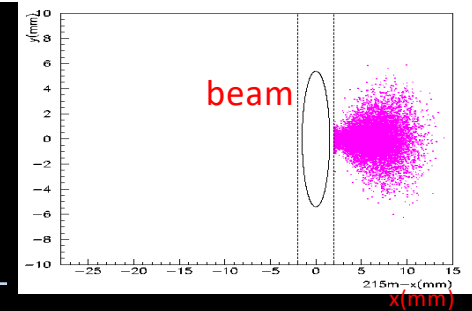


Silicon sensors with R-strips and ϕ -strips (2048 strips per sensor)

Sensor characteristics:

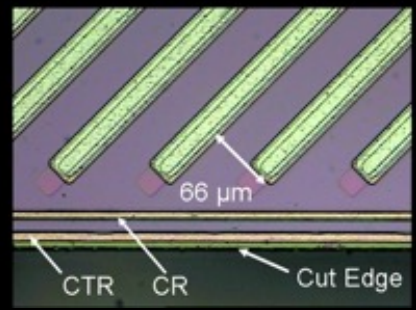
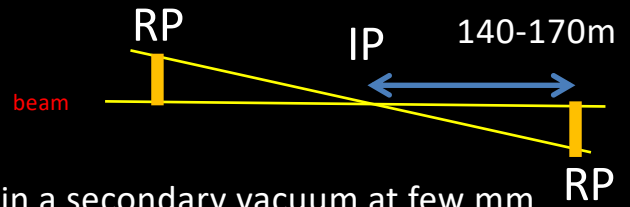
- 300 μm thick
- $8\text{mm} < \text{radius} < 42.2\text{mm}$
- $40\ \mu\text{m} < \text{pitch} < 101.6\ \mu\text{m}$
- radiation hard design:
 - oxygenated silicon
 - n-on-n type

TOTEM Roman Pots

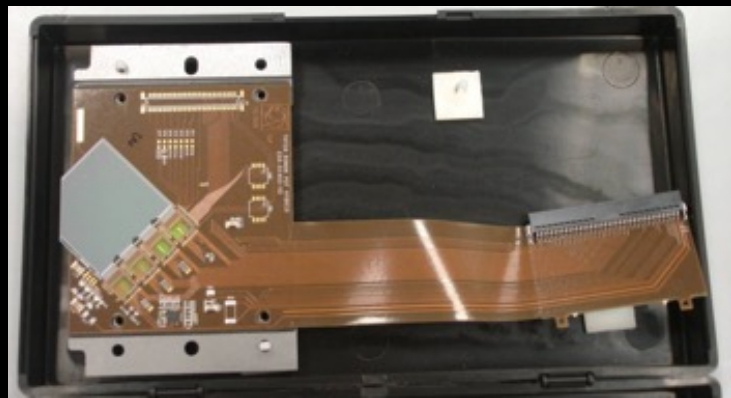
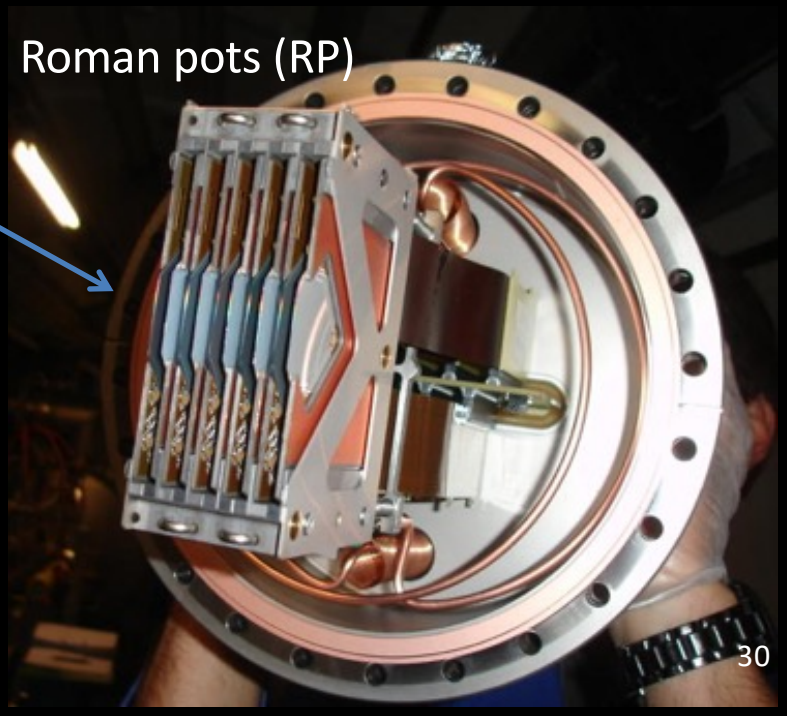


Totem measures the elastic scattering and the Total Cross Section at the LHC.

- Roman Pots are inserted in the beam pipe at 140-170m from the CMS experiment on both sides
- Standard planar technology is placed in a secondary vacuum at few mm from the beam



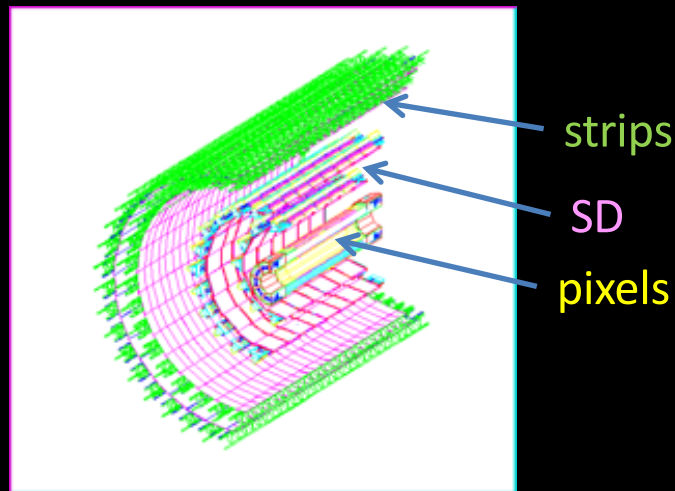
- Edge width 50μm at few mm from the beam



ALICE silicon drift detectors

G. Batigne IFAE

Cinzia Da Via, Uni. Manchester IEEE NPSS Workshop on Applications of Radiation Instrumentation, 2020



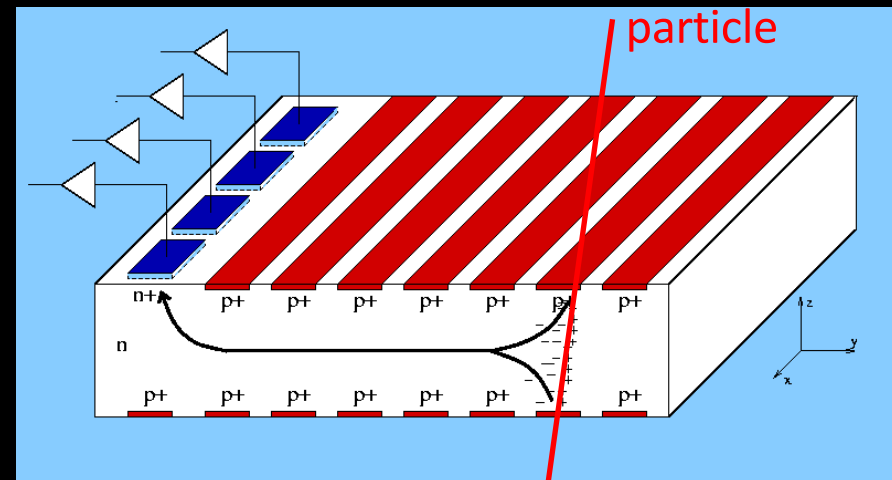
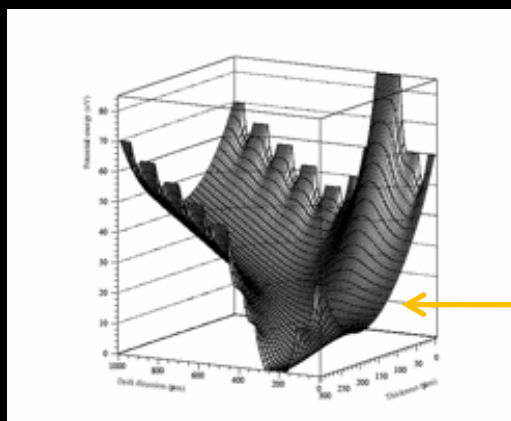
Position reconstruction : Centroid calculation

Position X : anods n+

Position Y : drift time (calibration of V_{drift})

dE/dx : Integral of the signal

Very low C and therefore very low noise!



p+ cathods on both side of the wafer :

- Depletion of the Silicon
- HV decreases toward the n+ anods

Drift field (Toboggan effect)

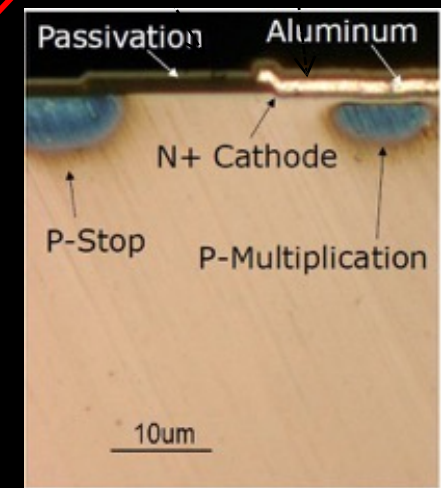
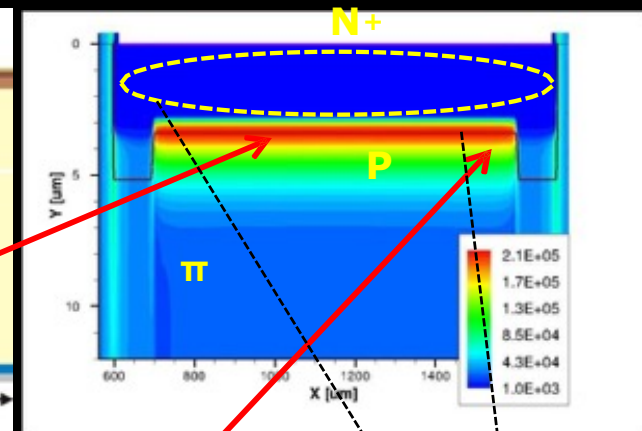
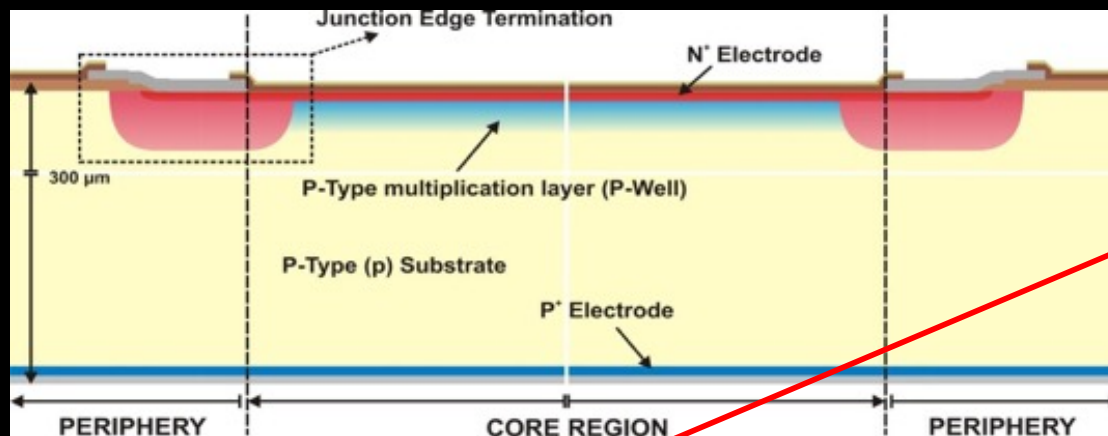
Last cathods below anods :

- kick-up voltage

LGAD Basics. Low Gain Detector

G. Pellegrini, Low Gain Avalanche Detectors

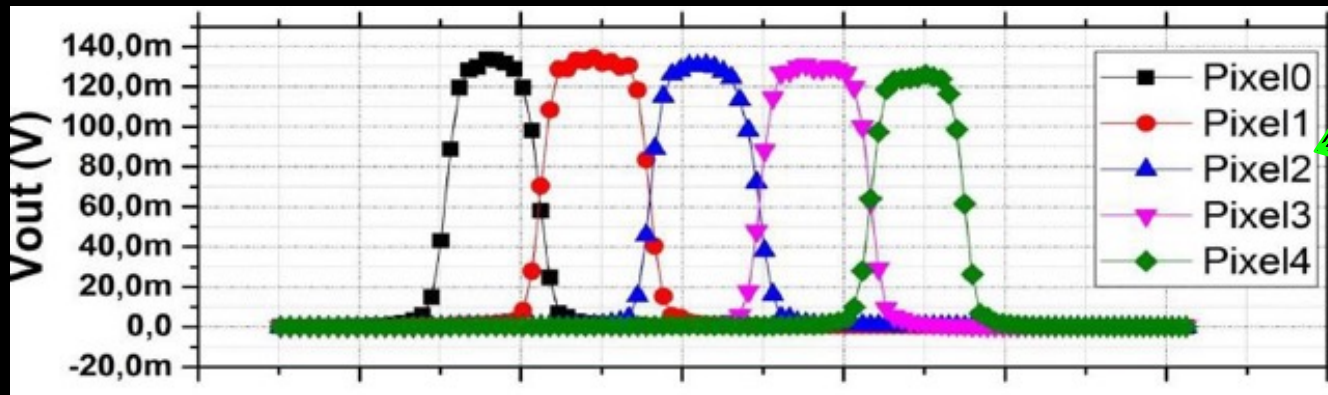
Cinzia Da Via, Uni. Manchester IEEE NPSS Workshop on Applications of Radiation Instrumentation, 2020



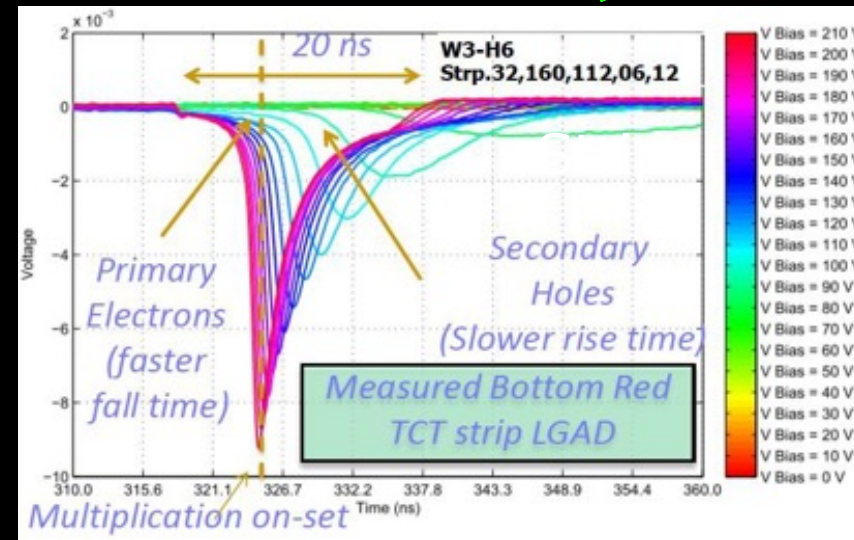
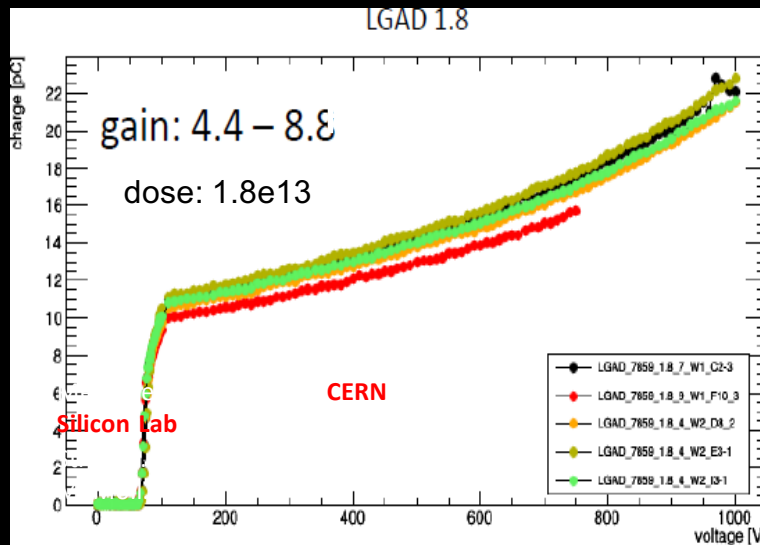
- **Core Region**
 - ✓ **Uniform electric field**, high enough to activate mechanism of **impact ionization** (multiplication)
- **Termination**
 - ✓ **High electric field** confined in the **core region**
- **Periphery**
 - ✓ **Dead region**. **Charges** should not be collected. **Reduction** of the surface **leakage currents**

LGAD Measurements

Cinzia Da Via, Uni. Manchester IEEE NPSS Workshop on Applications of Radiation Instrumentation, 2020



O. Alonso et al., presented at the PIXEL2016 workshop.

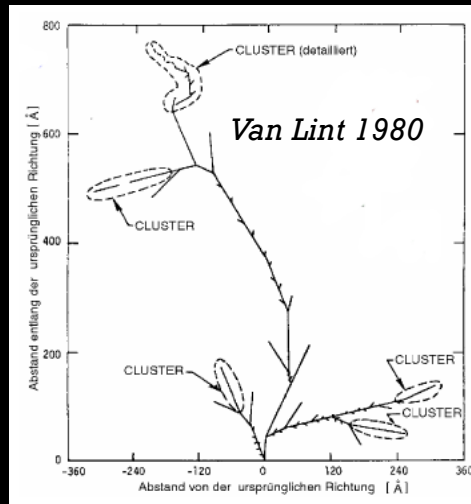


I. Vila, presented at the 28th RD50 workshop

What happens during irradiation to silicon detectors?

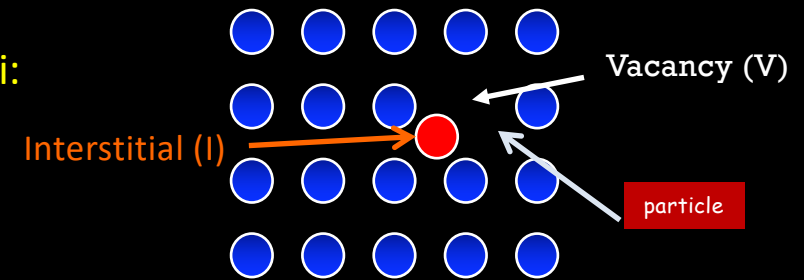
Defects formation in irradiated silicon

Cinzia Da Via, Uni. Manchester IEEE NPSS Workshop on Applications of Radiation Instrumentation, 2020

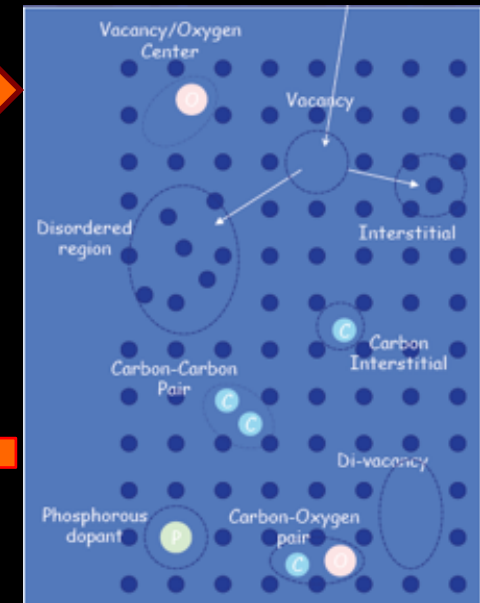
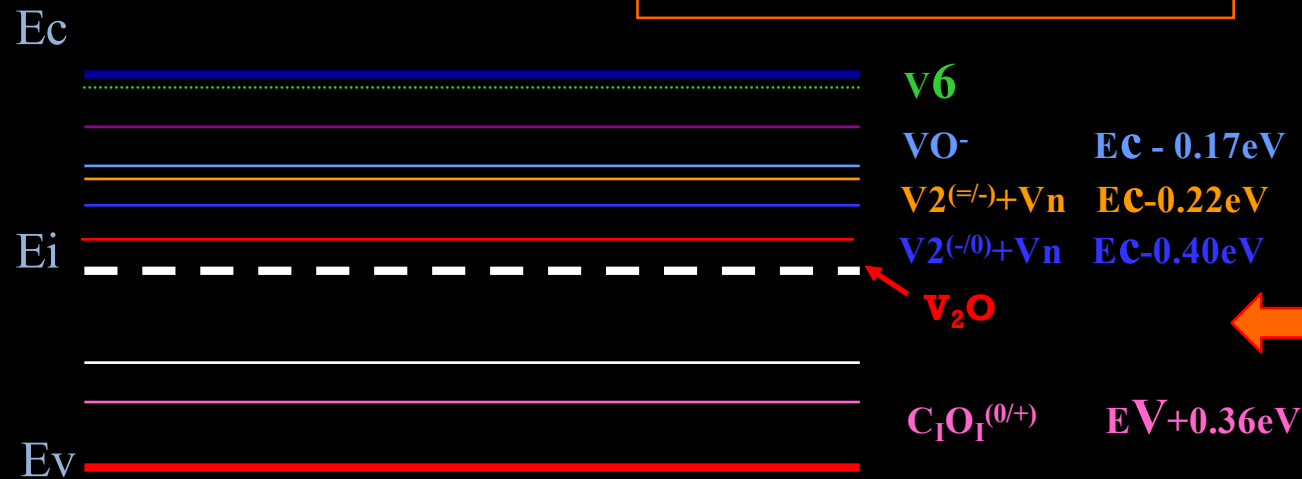


Primary Knock on Atom

Displacement thresholds in Si:
 Frenkel pair $E \sim 25\text{eV}$
 Defect cluster $E \sim 5\text{keV}$
 For X-Rays $E \sim 250\text{KeV}$



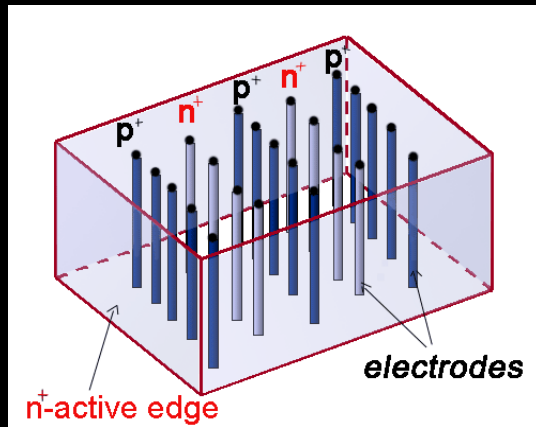
V, I MIGRATE UNTIL THEY MEET IMPURITIES AND DOPANTS TO FORM STABLE DEFECTS



Defects position in the bandgap

3D radiation sensors

Cinzia Da Via, Uni. Manchester IEEE NPSS Workshop on Applications of Radiation Instrumentation, 2020



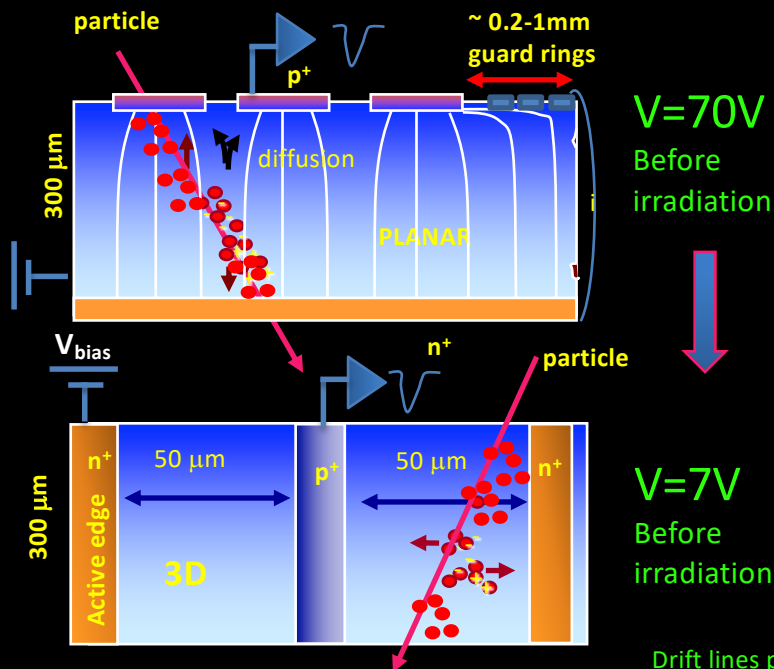
3D silicon detectors were proposed in 1995 by S. Parker, and active edges in 1997 by C. Kenney.

Combine traditional electronics processing and MEMS (Micro Electro Mechanical Systems) technology.

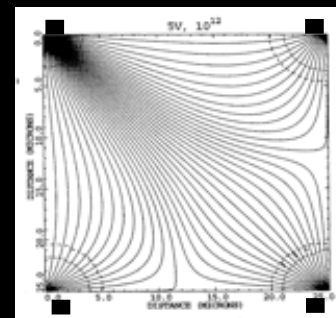
Electrodes are processed inside the detector bulk instead of being implanted on the wafer's surface.

The edge is an electrode! Dead volume at the edge < 5 microns!

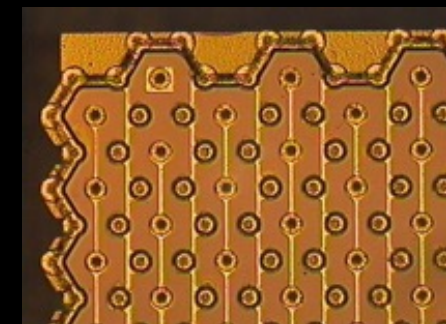
The electric field is parallel to wafer's surface: and smaller inter-electrode spacing: low bias voltage, low power, reduced charge sharing and high speed – for the same wafer thickness



Drift lines parallel to the surface



MEDICI simulation of a 3D structure

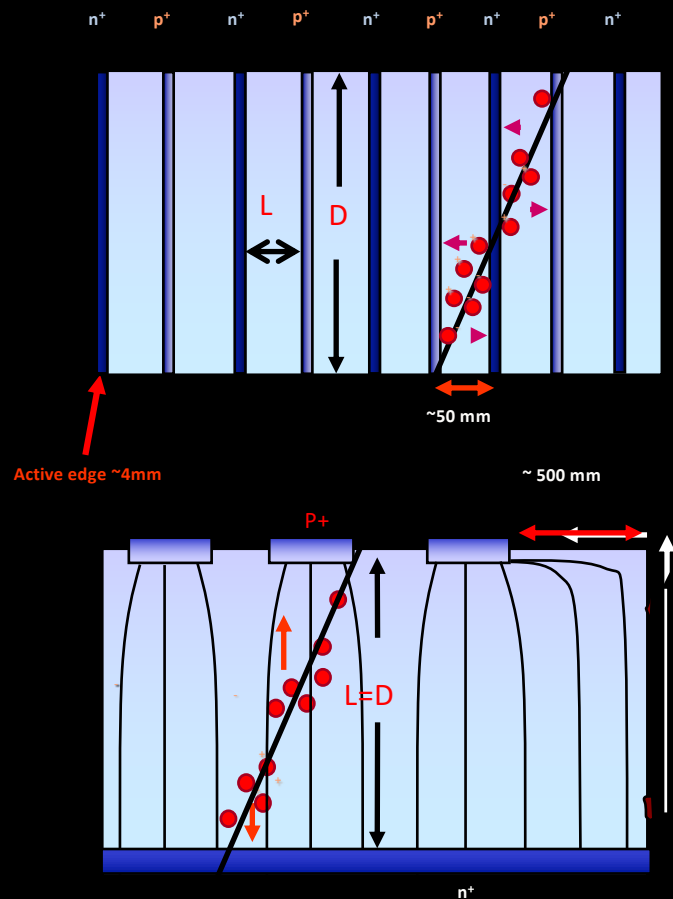


3D is “geometrically” radiation hard at low V_{bias} (hence low power)

Ramo's theorem

3D

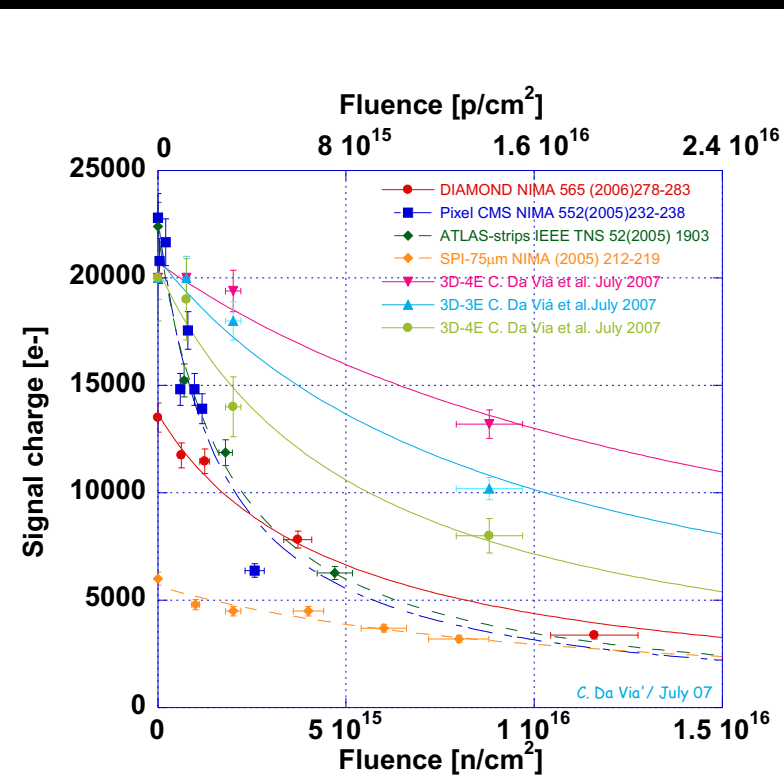
particle



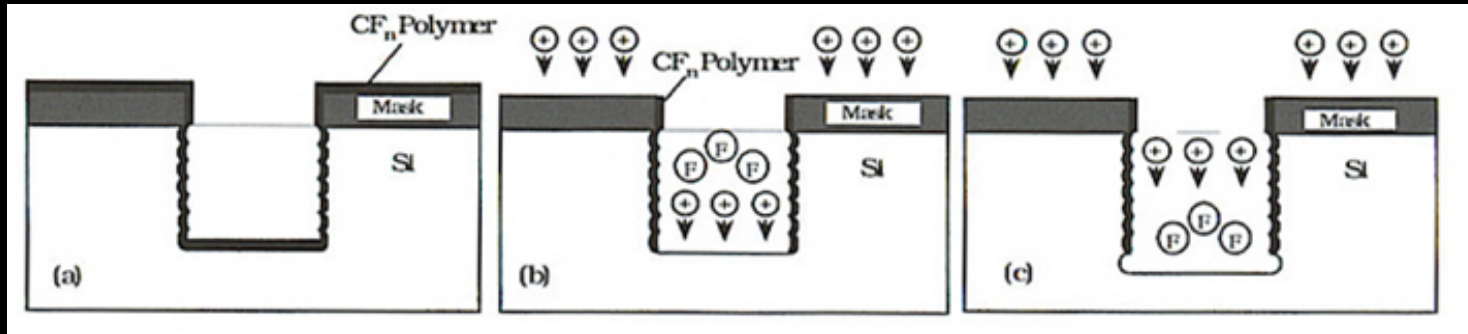
- 3D 4E
- 3D 3E
- 3D 2E
- Diamond
- Thick Si
- Thin Si

$$\lambda = v_D \cdot \tau$$

$$S = \frac{\lambda}{L} \left[1 - \exp\left(-\frac{x}{\lambda}\right) \right]$$

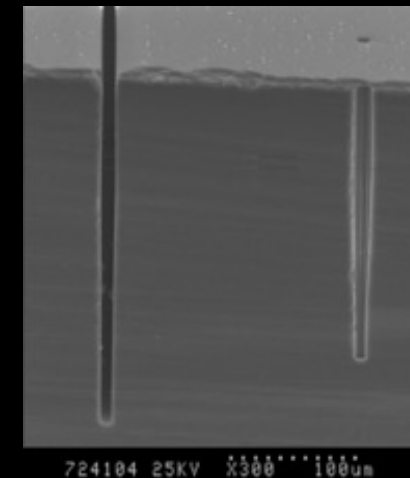


The key to fabrication: plasma etching



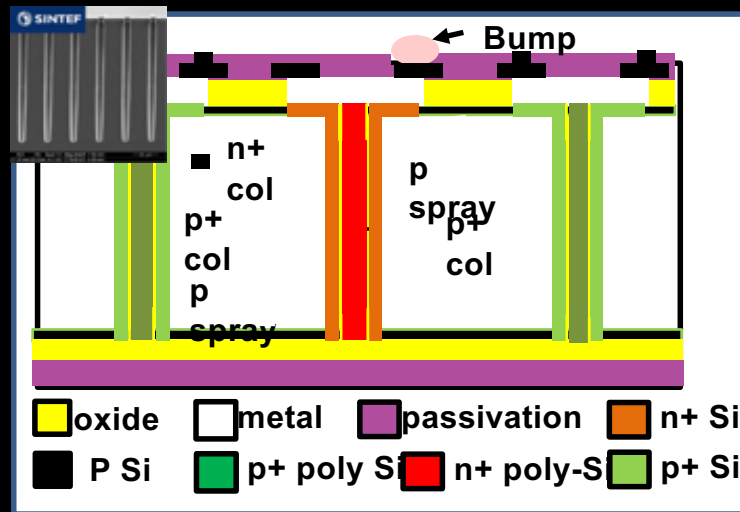
BOSCH PROCESS: alternating passivation (C_4F_8) and etch cycles (SF_6);

- ❖ Within the plasma an electric field is applied perpendicular to the silicon surface.
- ❖ The etch cycle consists of fluorine based etchants which react with silicon surface, removing silicon. The etch rates are $\sim 1-5\mu\text{m}/\text{minute}$.
- ❖ To minimize side wall etching, etch cycle is stopped and replaced with a passivation gas which creates a Teflon-like coating homogenously around the cavity. Energetic fluorine ions, accelerated by the e-field, remove the coating from the cavity bottom but NOT the side walls.



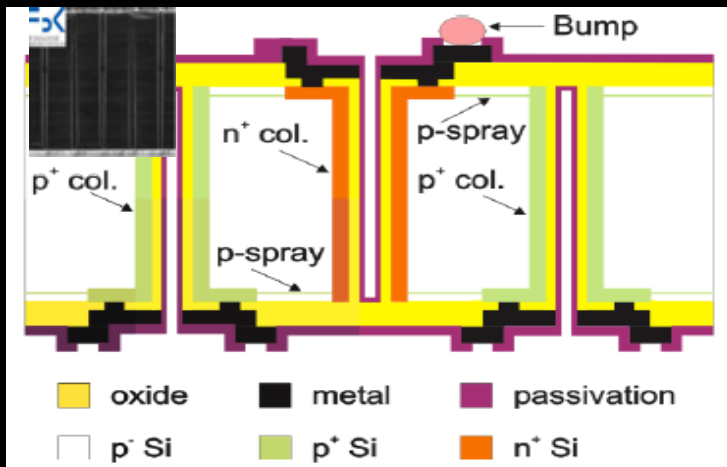
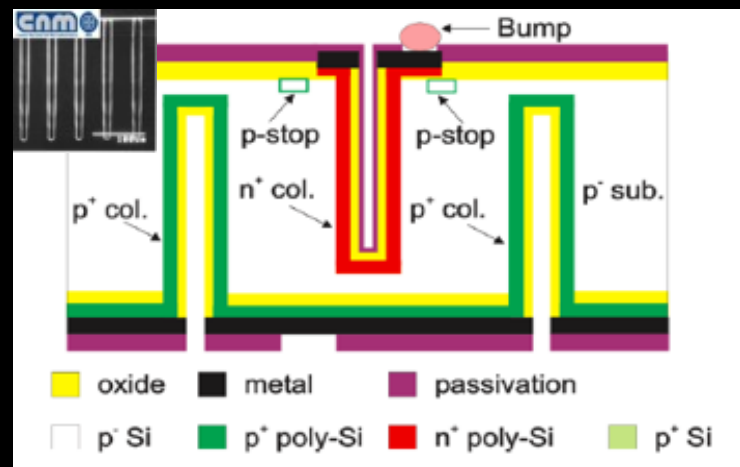
Existing 3D designs

Cinzia Da Via, Uni. Manchester IEEE NPSS Workshop on Applications of Radiation Instrumentation, 2020



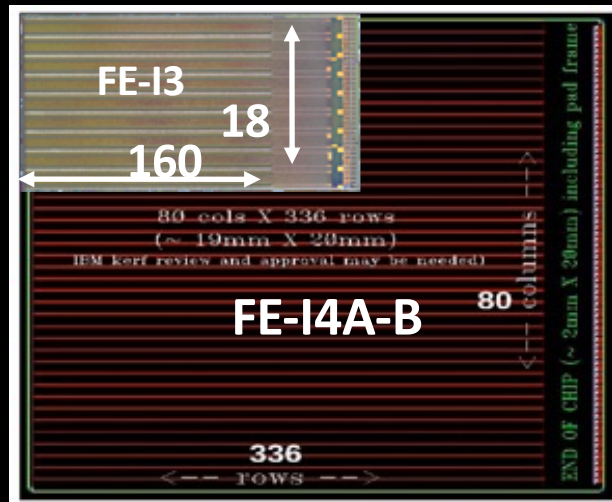
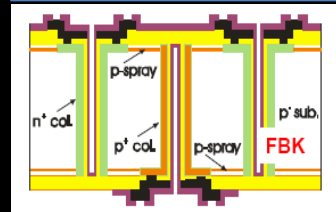
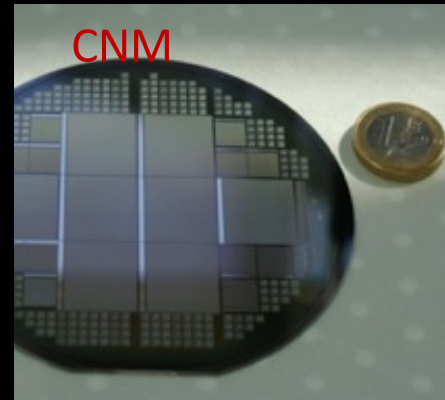
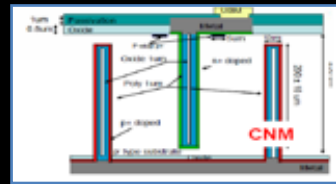
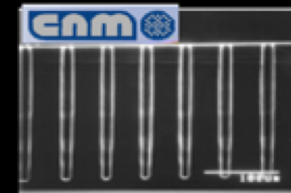
Single side, full 3D with active edges requires a support wafer which is removed later

Double sided full or partially through 3D with slim-fences (~200um)

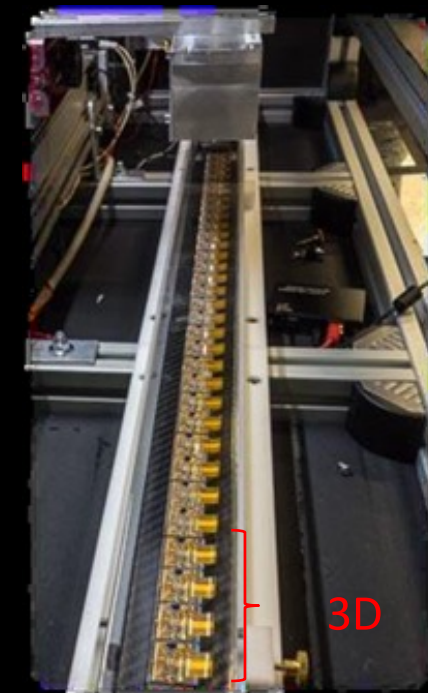
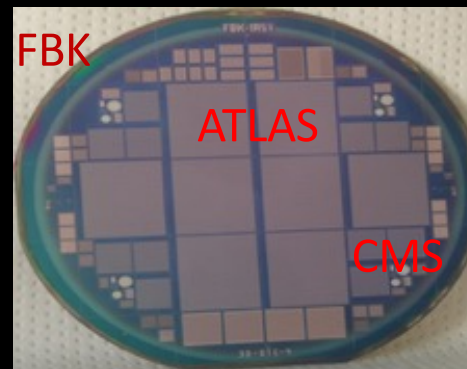


3D sensors are installed in the LHC since 2014
 Upgrade in the ATLAS –Insertable B-Layer (IBL)
 >300 sensors fabricated and now being loaded to cover 25% IBL

NIMA 694 (2012) 321–330

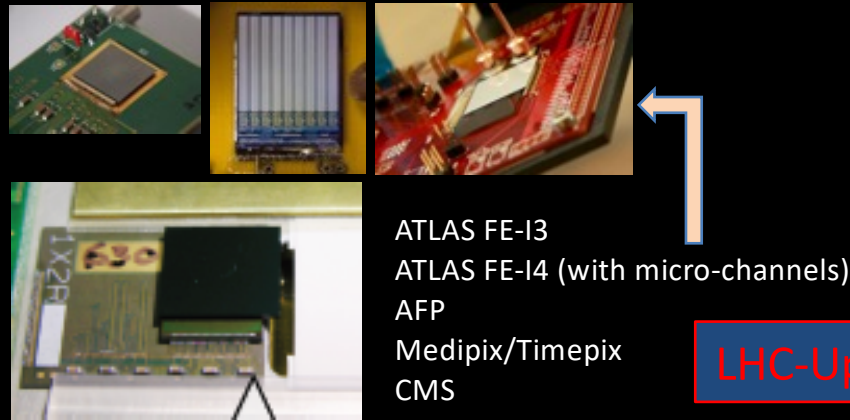


2x2cm²
 250x50um², 26880 pixels



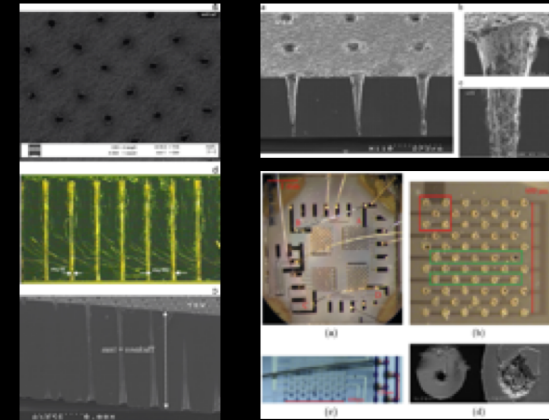
"3D" Radiation Detectors and Active Edges

Cinzia Da Via, Uni. Manchester IEEE NPSS Workshop on Applications of Radiation Instrumentation, 2020

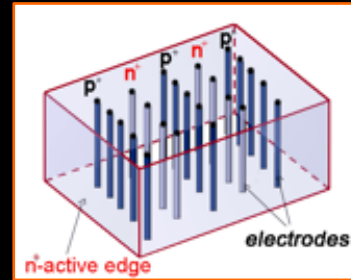


LHC-Upgrades

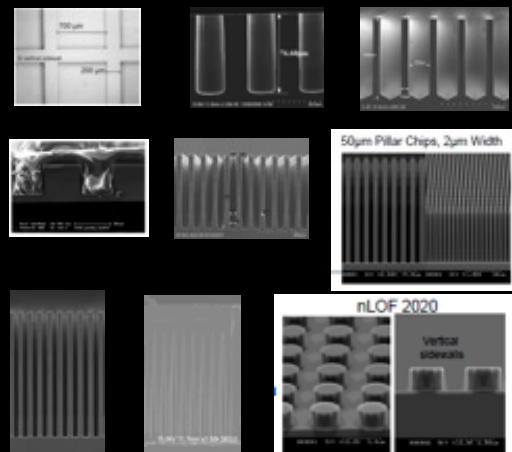
- GaAs
- CdTe
- Diamond



Consolidated ← Silicon +ASIC
Silicon +Converter



→ New Materials
Emerging
New Shapes



Neutron detectors

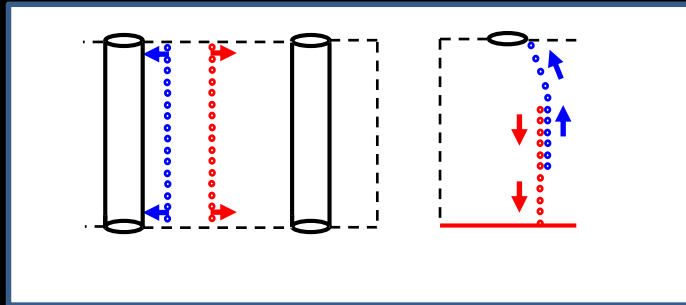
3D

- Core shell
- Trench
- Curved
- Edge
- Ring..

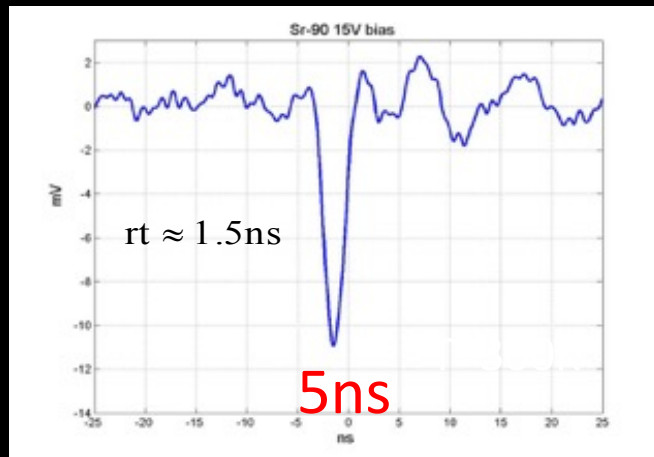


3D Speed Properties

3D Tests with 0.13 mm CMOS Amplifier chip
(A Kok, S. Parker, C. Da Viá, P. Jarron,
M. Depeisse, G. Anelli), fabricated at Stanford
By J. Hasi, C. Kenney

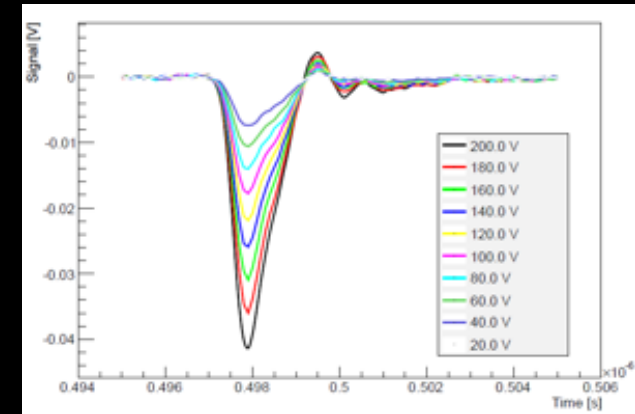


- ❖ Short collection distance
- ❖ High average e-field at low V_{bias}
- ❖ Parallel charge collection

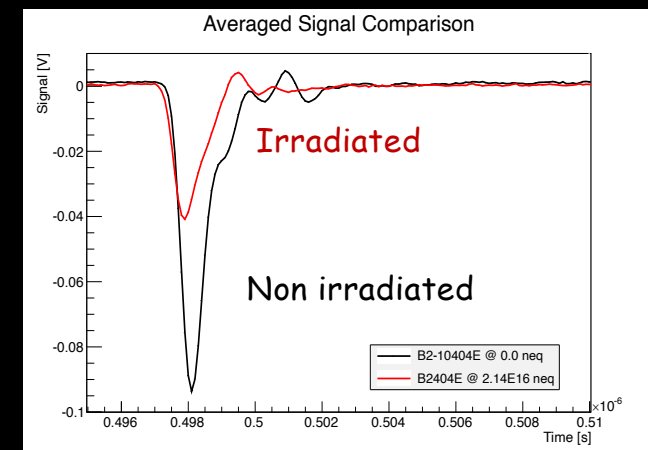


Raw oscilloscope
Trace rt is dominated
by amplifier

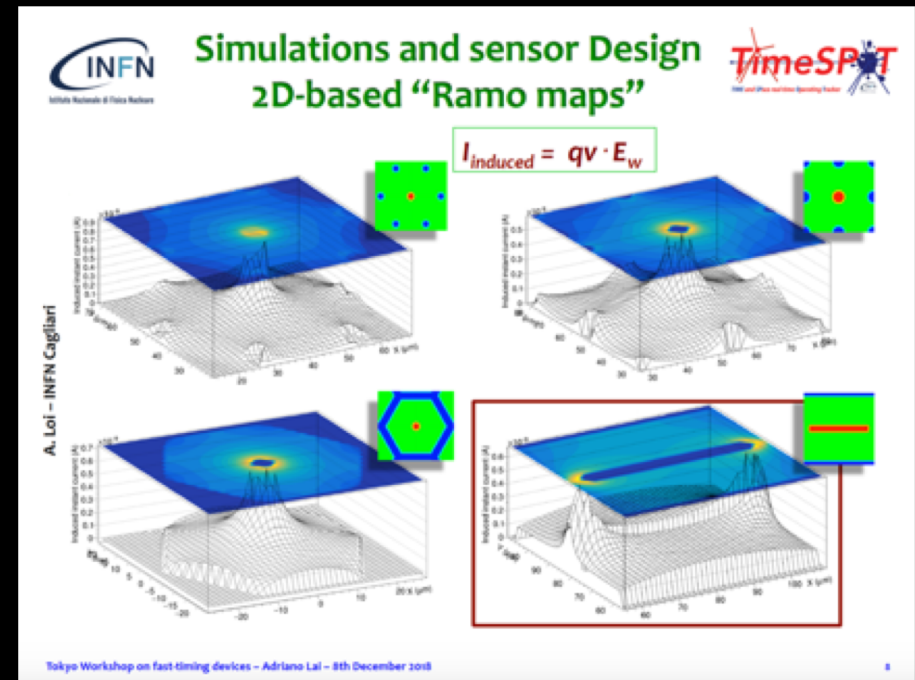
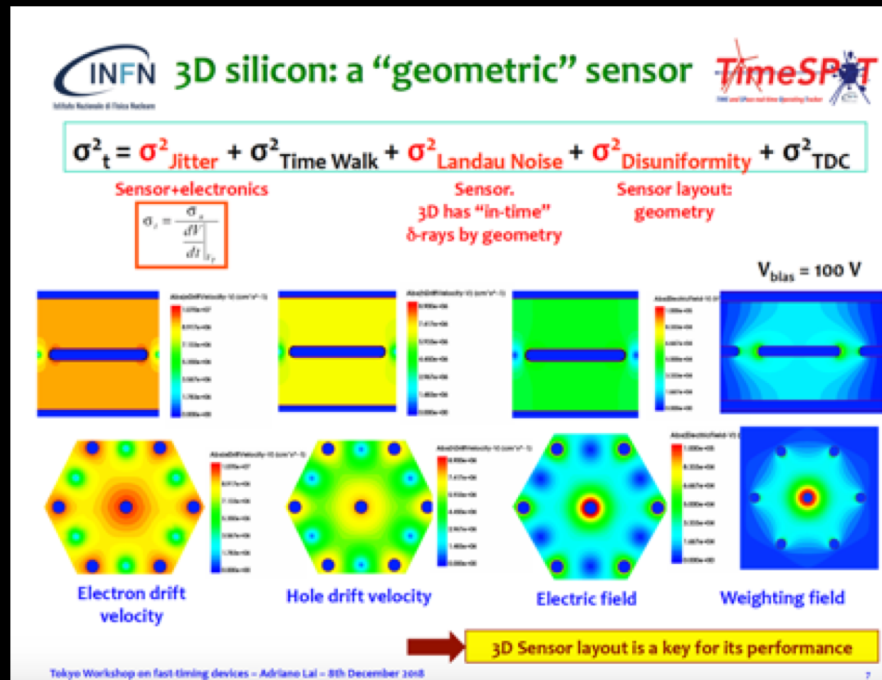
3D Inter-electrode
spacing = 56 μm



After irradiation $2 \times 10^{16} \text{ ncm}^2$



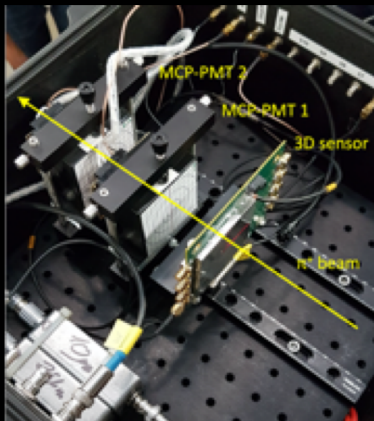
3D with small IES and trench electrodes



Recent Trench electrodes time response without multiplication

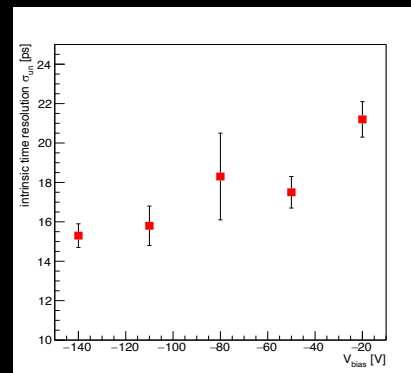
TimeSpot Collaboration
INSTANT Collaboration

Tests of timing performance of silicon sensors designed for timing by our group (3D-trench sensors).



Test beam setup

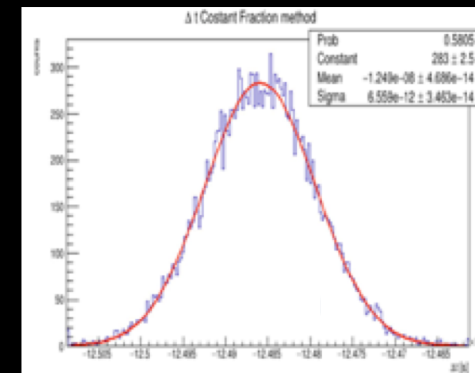
Intrinsic (sensor only) time resolution s_t reaches 15 ps and ≈ 20 ps if the F/E electronics contribution is included



Intrinsic trench sensor jitter, with MIP beam

$$\sigma_t \approx 15 \text{ ps}$$

New electronics development (discrete components) yield better performance!



1030 nm laser, single spot, 1 MIP equiv. charge deposit

$$\sigma_t \approx 6.5 \text{ ps}$$

```

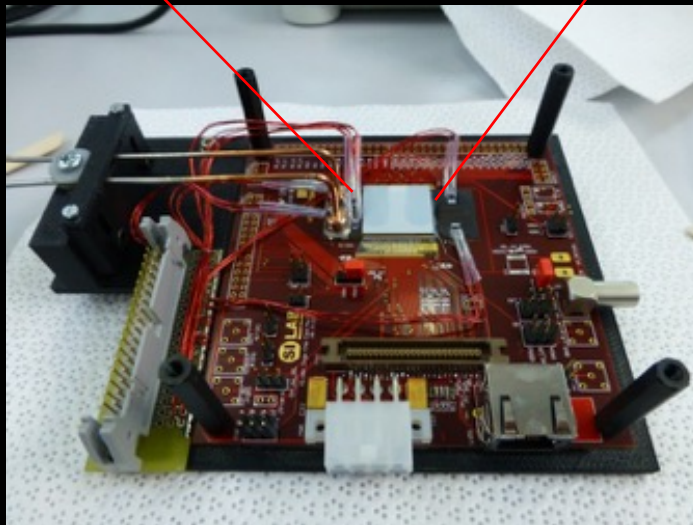
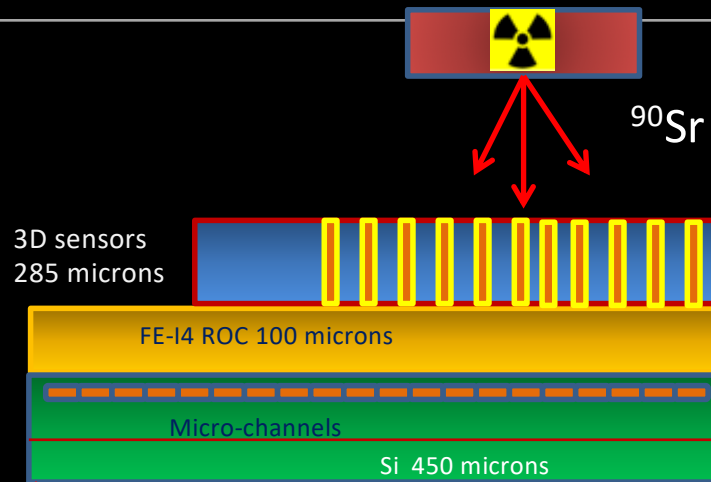
deci [d] 0.1
centi [c] 0.01
milli [m] 0.001
micro [μ] 0.000001
nano [n] 0.000000001
pico [p] 0.000000000001
femto [f] 0.000000000000001
atto [a] 0.000000000000000001
zepto [z] 0.0000000000000000001
yocto [y] 0.00000000000000000001
    
```

Usual timing is 1-2 ns !

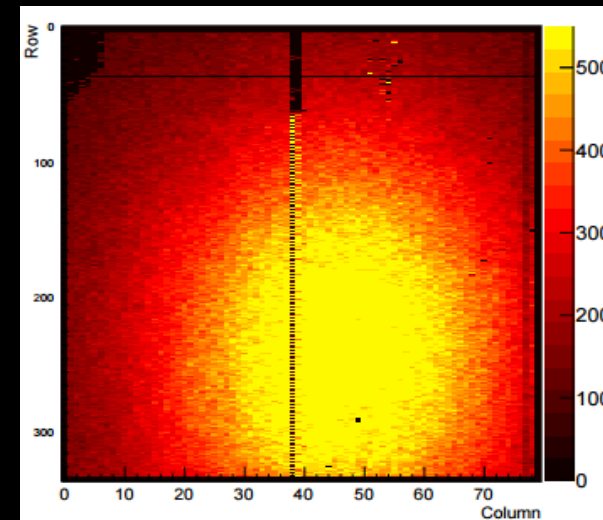
3D Vertically Integrated Module with CO₂ internal cooling

C. Da Via, F. Munoz-Sanchez, N. Dann,
D. Hellesmidht, P. Petagna, G. Romagnoli
Paper in preparation

Cinzia Da Via, Uni. Manchester IEEE NPSS Workshop on Applications of Radiation Instrumentation, 2020



- 3D silicon : CNM double side 285 um thick IBL qualification batch
- FE-I4A: thinned to 100um at IZM
- Si-Si micro-channels
designed by CERN PH-DT,
produced by PH-DT in EPFL CMi cleanroom,
direct bonding CSEM
- Glue: 2-components
Masterbond EP37-3FLFAO



Applications: Silicon Micro-dosimetry

for Cancer Therapy, Space Radiation Monitoring

Mimic Project
A. Kok et al SINTEF

Microdosimetry measures the stochastic energy deposition events at cellular level

Radio-Biological Effectiveness (RBE) depends on linear energy transfer (LET or Lineal Energy) which is different for different radiation type. **Average chord length $\langle l \rangle$** independent on radiation direction

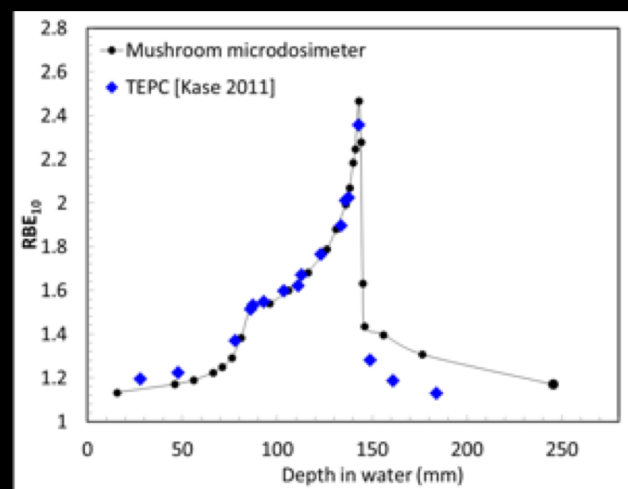
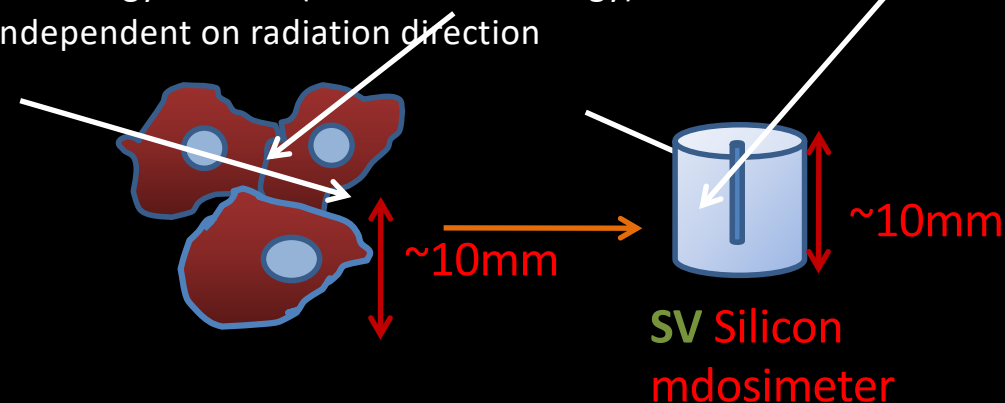
❖ **Mixed Field** detection in a small sized array of cell-like elements of well defined Sensitive volume **SV** is required to precisely determine RBE

❖ Silicon Dose Equivalent can be determined From the lineal Energy Spectra and the tissue equivalent dose D_{TE} . Quality factors **Q** determined Experimentally.

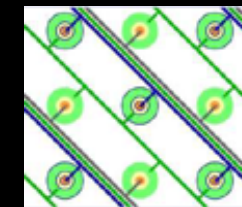
$$D_{si} = D_{TE} S_{Si}/S_{TE}$$

$$\text{Dose equivalent } H = Q D_{si}$$

Use array of 3D sensors with central n^+ electrode surrounded by p^+ trench to define cellular size sensitive volume



Dose distribution $d(y)$

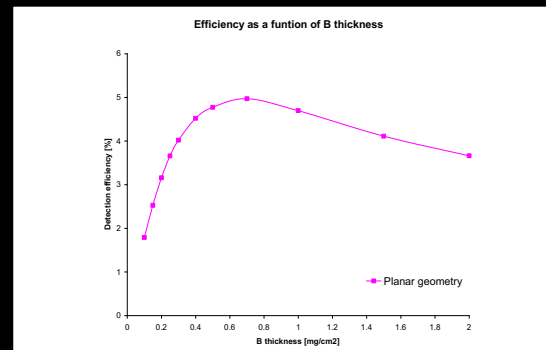
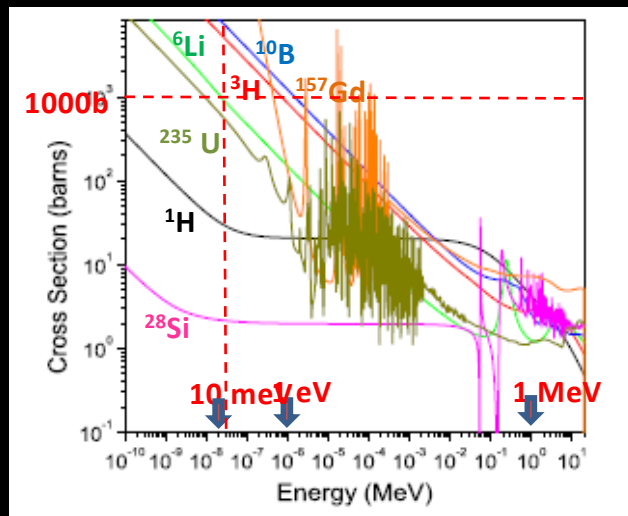
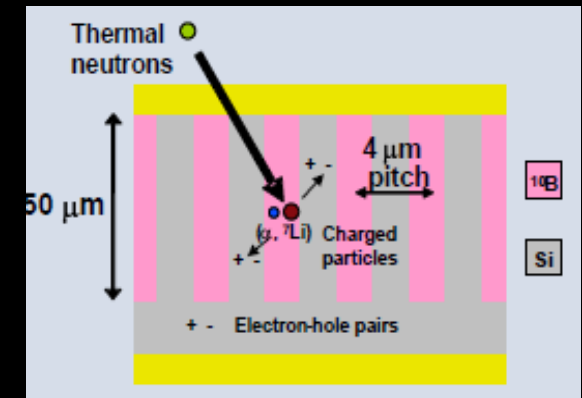
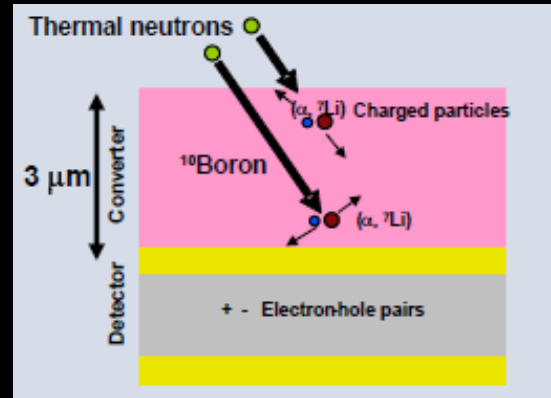


Povoli et al TREDI 2017 and A. B. Rosenfeld et al., "New 3D Mushroom microdosimeter for RBE studies in passive scattering and pencil beam scanning heavy ion therapy, IEEE NSS 2016

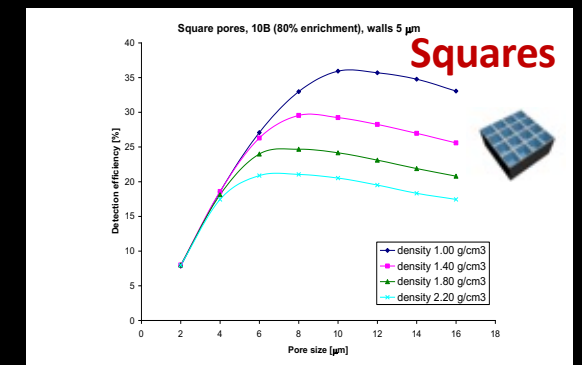
Applications: High Efficiency Neutron Detection

Uher et al. Nuclear Instruments and Methods in Physics Research A 576 (2007) 32–37

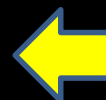
- Silicon is not sensitive to neutrons but is a well known radiation detector
- Need neutron reactive converter materials usually deposited on the surface thin films or different geometries
- With reference to ^{10}B converter:
 - 90% capture in $43\ \mu\text{m}$
 - Range of reaction products $2\text{-}5\ \mu\text{m}$



Amorphous ^{10}B , enrichment 80%
Efficiency < 5%



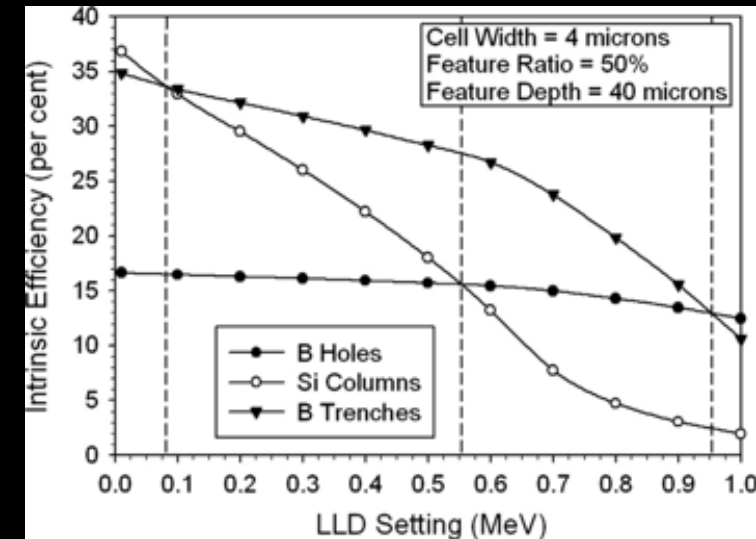
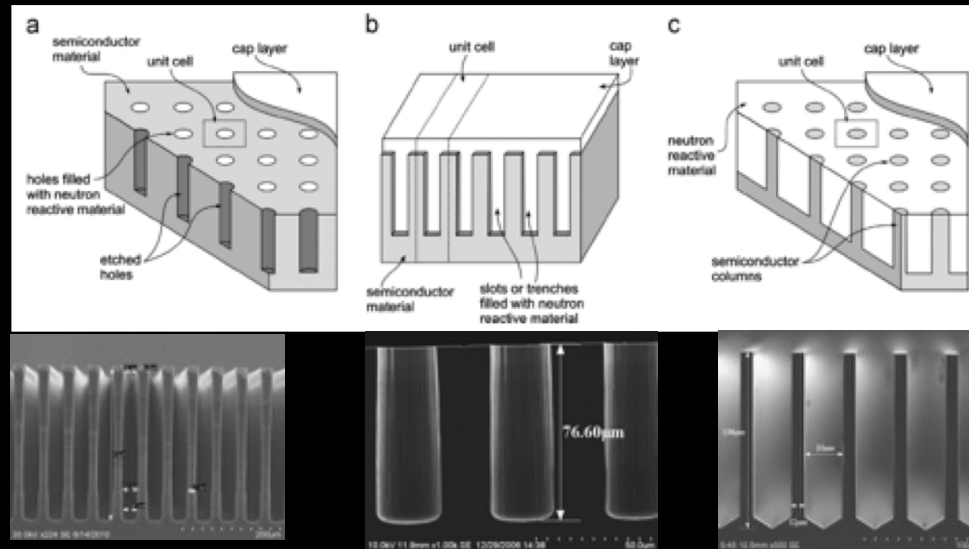
Efficiency up to 36%



Neutron cross sections of some common n-reactive materials

Micro-structured Semiconductor Neutron Detectors (MSND)

D. McGregor et al., J. Crystal Growth 379 (2013) 99



- Extended interaction surface, and higher probability for reaction products to enter the semiconductor
- Different shapes and geometries

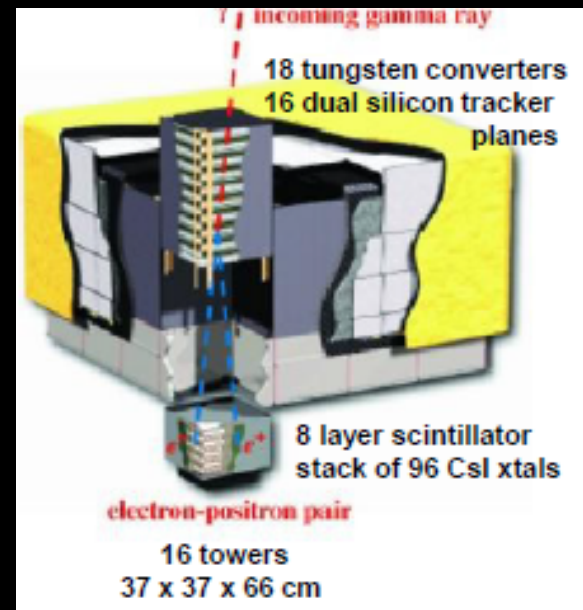
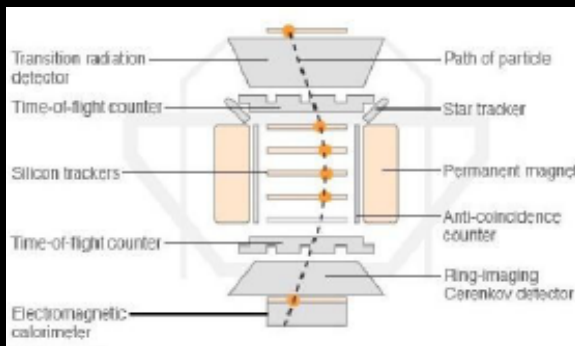
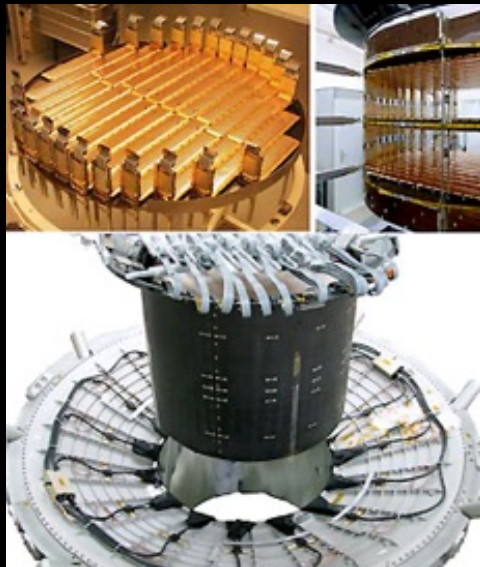
Comparison of efficiencies as a function of feature size, as measured by its cell fraction, for hole, trench and column designs with unit cell dimensions of 4 μm and feature depths of 40 μm. ¹⁰B is the back fill material and the LLD was set for 300keV

Maximum efficiencies reported ~50%

Applications: Detectors in Space

Cinzia Da Via, Uni. Manchester IEEE NPSS Workshop on Applications of Radiation Instrumentation, 2020

AMS (Alpha Magnetic Spectrometer)
on ISS particle physics experiment in space
to measure antimatter in cosmic rays



FERMI Large Area Telescope

Gamma-ray detector

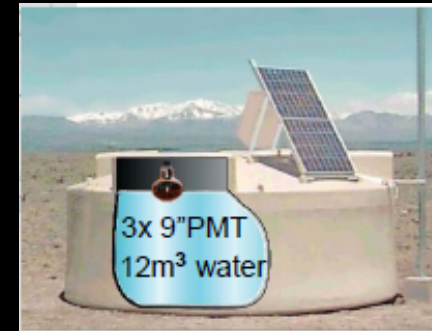
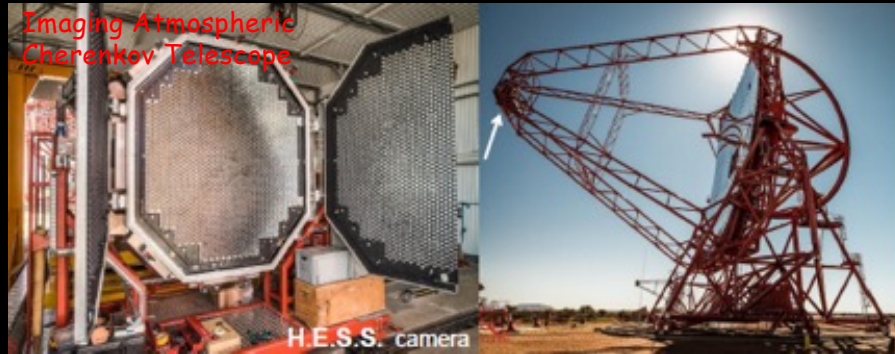
Cycle of pulsed gamma rays from the Vela pulsar.
Constructed from photons detected by Fermi's Large Area Telescope.

Roger Romani

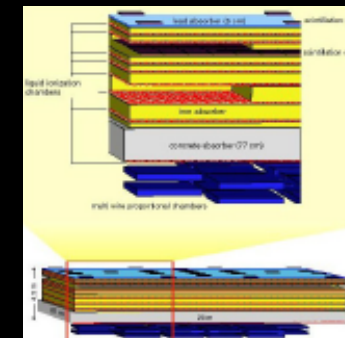


Applications: Ground Detectors – Cosmic Rays

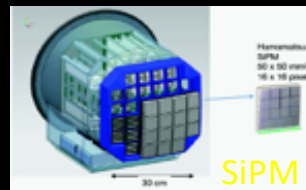
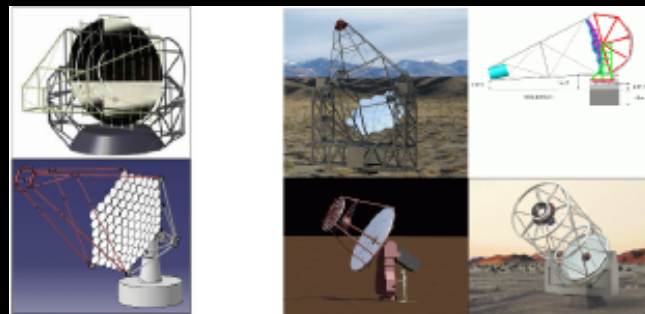
Cinzia Da Via, Uni. Manchester IEEE NPSS Workshop on Applications of Radiation Instrumentation, 2020



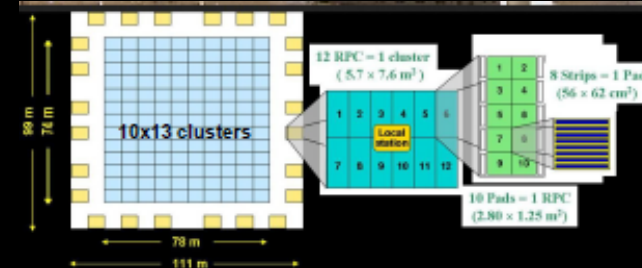
Pierre Auger Observatory
UHE 10²⁰eV
1600 water
Cherenkov detectors



KASCADE-Grande
200x200 m² scint. array
20x16 m² h. calorimeter
128 m² muon tracker



ARGO-YBJ -RPCs



SST 70x (S) : > few TeV
>5 m², >8° FoV, <0.25° pxl

MST 25x (S) : 0.2-10 TeV
>88 m², >7° FoV, <0.18° pxl

LST 4x (S) : 20 GeV - 1 TeV
>330m², >4.4° FoV, <0.11° pxl size

Camera Options

Follow-up project LHAASO

Applications: Environmental Radiation Monitoring

Cinzia Da Via, Uni. Manchester IEEE NPSS Workshop on Applications of Radiation Instrumentation, 2020

Gamma Dose Rate (GDR) networks in Europe



1cm³ coplanar grid (Cd,Zn)Te detector

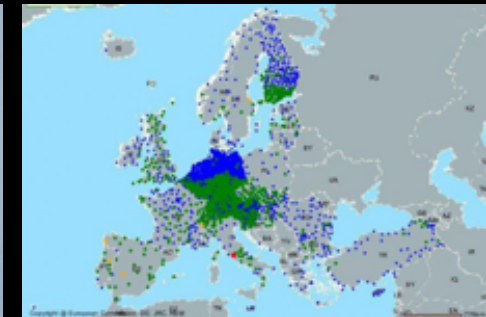


Broken mountain

German Network
1800 GDR stations
to perform gamma
Spectrometry and
Create contamination
Map for long-lived
radionuclides



Inter-calibration facility (INTERCAL) on Schauinsland mountain (1200 m) since 2007

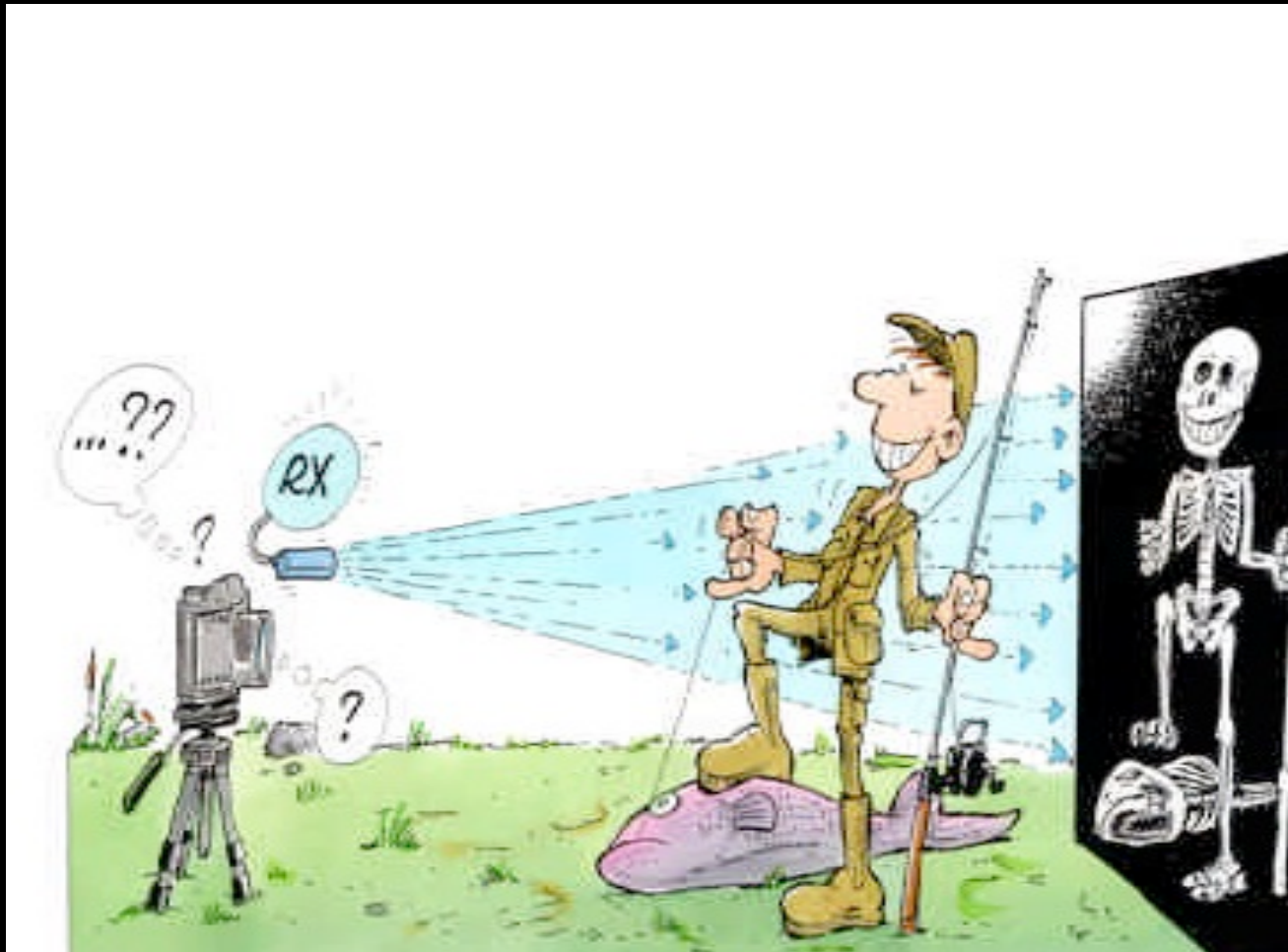


European countries established GDR networks during the cold war period and improved these networks after the Chernobyl accident in 1986.

Monitoring of:

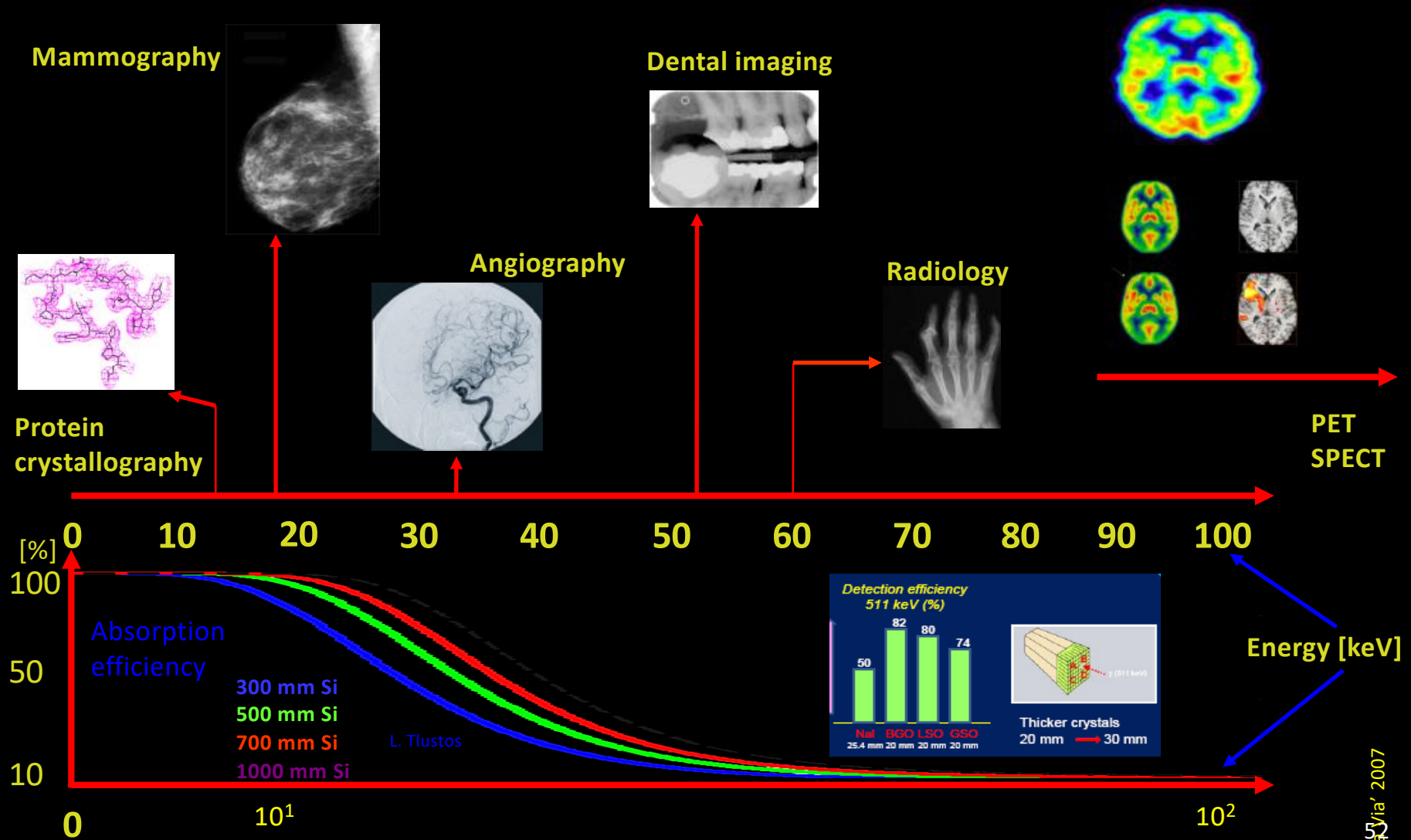
- nuclear facilities
- atomic bomb scenarios
- terroristic attacks

Applications: Medical Imaging



X-ray energy of the most common medical and biological applications

Cinzia Da Via, Uni. Manchester IEEE NPSS Workshop on Applications of Radiation Instrumentation, 2020



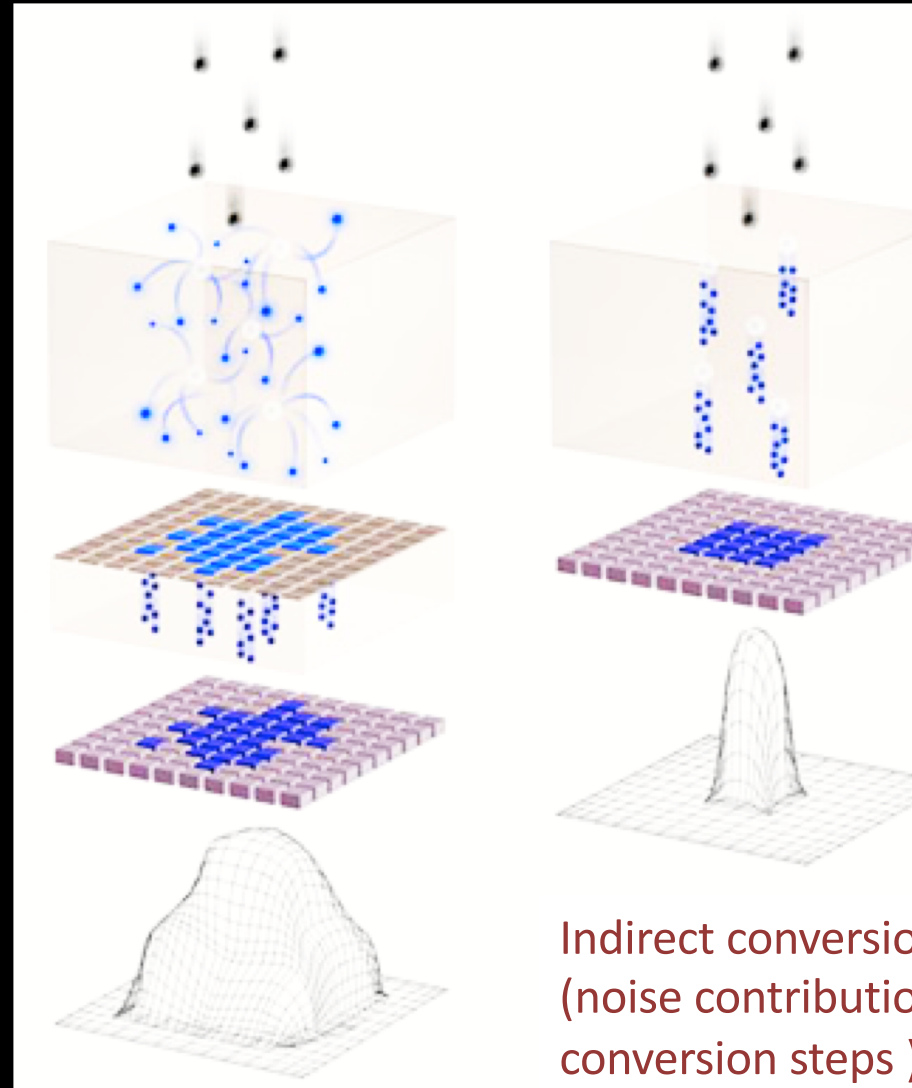
Direct / indirect conversion

The target is to reduce the dose to the patient!

Scintillator
Gadox, YAG CsI
(high Z)
Photodiode/ CCD
electronics

electronics

Sampled image



X-rays

Direct conversion
Si, Ge, CdTe,
GaAs, Se

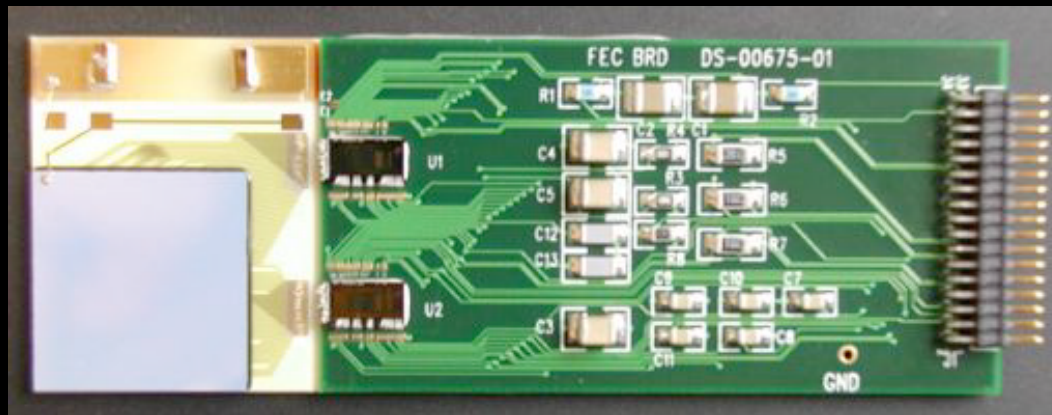
Sampled image

Indirect conversion implies lower DQE
(noise contribution from the two
conversion steps)

High Z semiconductors: CdTe and CdZnTe

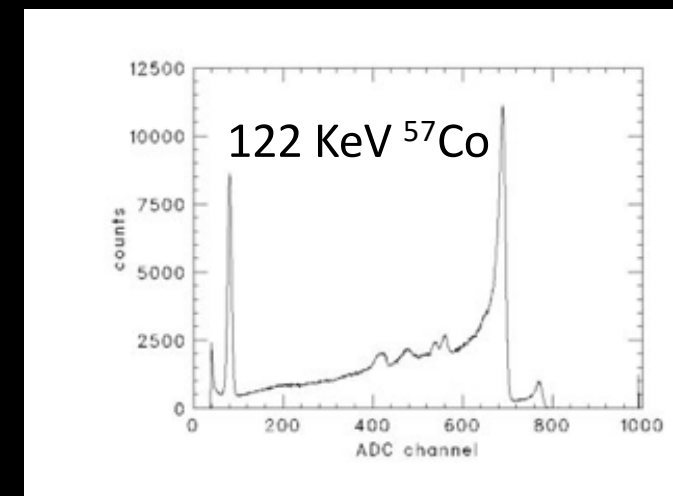
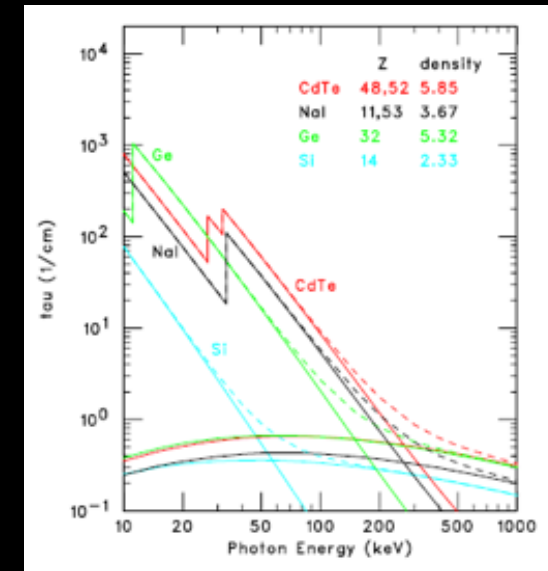
Taka Tanaka (SLAC/KIPAC)

- High detection efficiency
- Poly-crystalline material
- Poor uniformity
- Very high resistivity (semi-insulating)
- Low leakage current



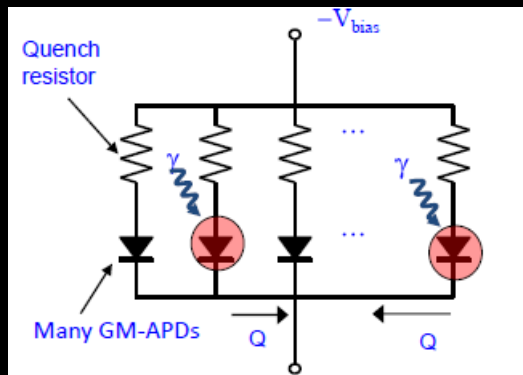
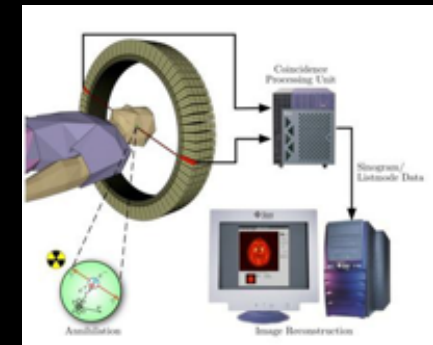
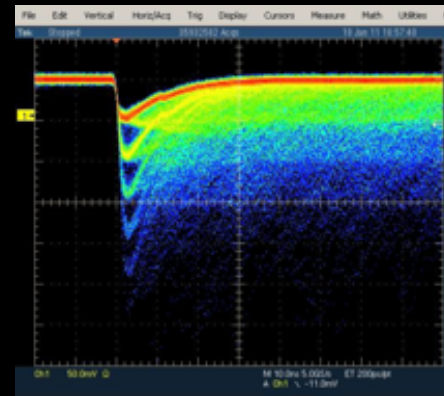
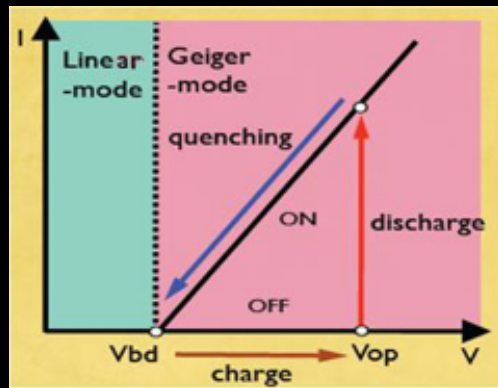
area: 18 " 18 mm²
 thickness: 0.5 mm
 pixel size: 2 " 2 mm²,
 64 ch, cathode side
 guard ring: 1 mm width

Fabricated at IDEAS
 Norway

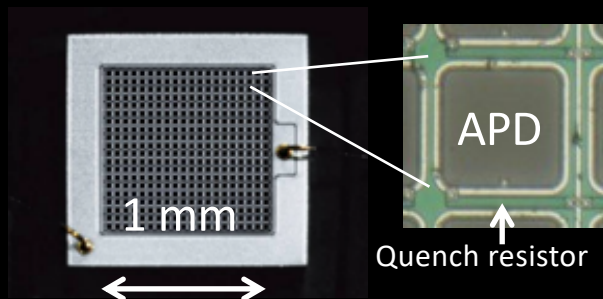


Indirect Conversion: Scintillators and Silicon Photomultipliers (SiPm, GM-APD, MPPC...)

Cinzia Da Via, Uni. Manchester IEEE NPSS Workshop on Applications of Radiation Instrumentation, 2020



- SiPm requires a special doping profile to allow a high internal field ($>10^5$ V/cm) which generates avalanche multiplication
- APD cell operates in Geiger mode (= full discharge), however with (passive/active) quenching.
- The avalanche formation is intrinsically very fast (100ps), because confined to a small space.
- High Gain $G \sim 10^5 - 10^6$ at rel. low bias voltage (<100 V)
- G is Sensitive to temperature and voltage variations
- Fill factor still low due to quench resistor on the surface (but work in progress to solve this)



Applications in PET

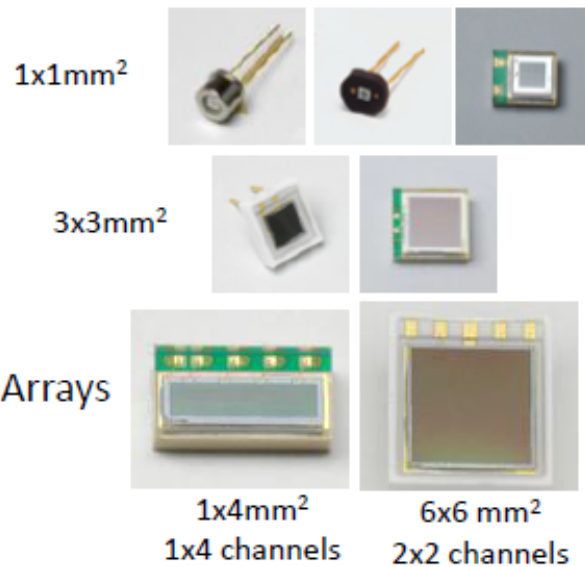
coincidence of two 511 keV photons define a line of record.

- Take projections under all angles
- (2/3D) Tomographic reconstruct of data

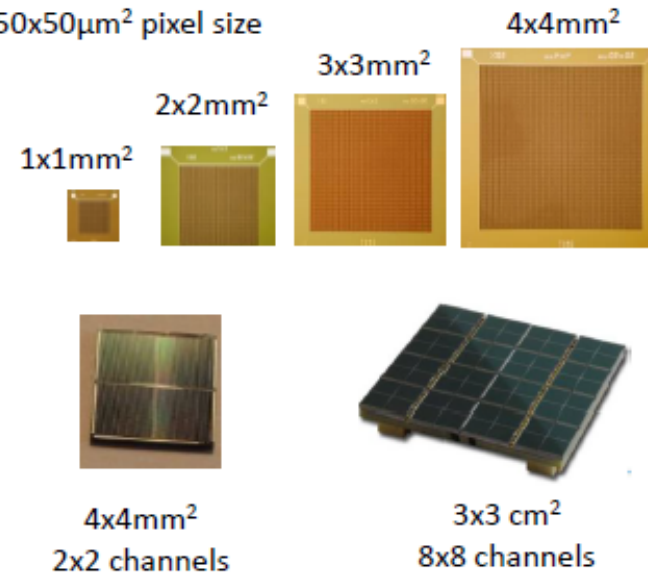
SiPm Commercial Activity

From C. Joram CERN

Hamamatsu HPK (<http://jp.hamamatsu.com/>)
25x25 μm^2 , 50x50 μm^2 , 100x100 μm^2 pixel size



FBK-IRST
50x50 μm^2 pixel size



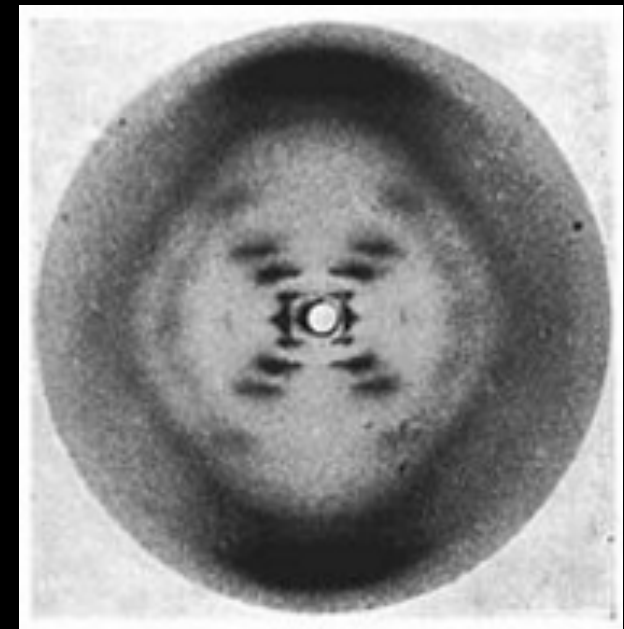
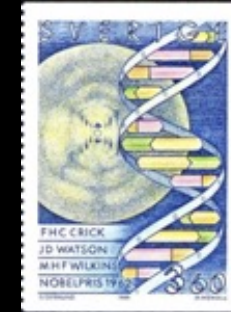
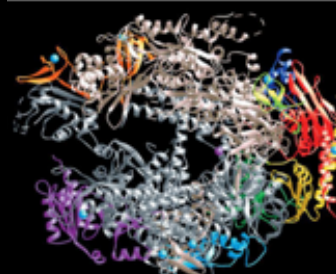
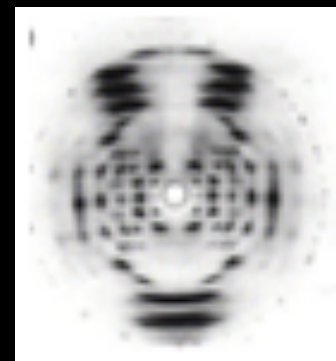
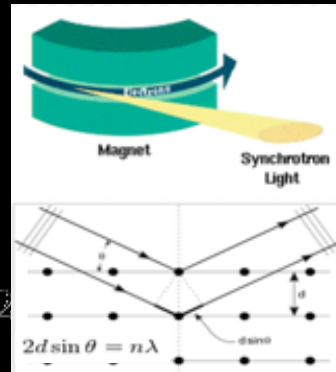
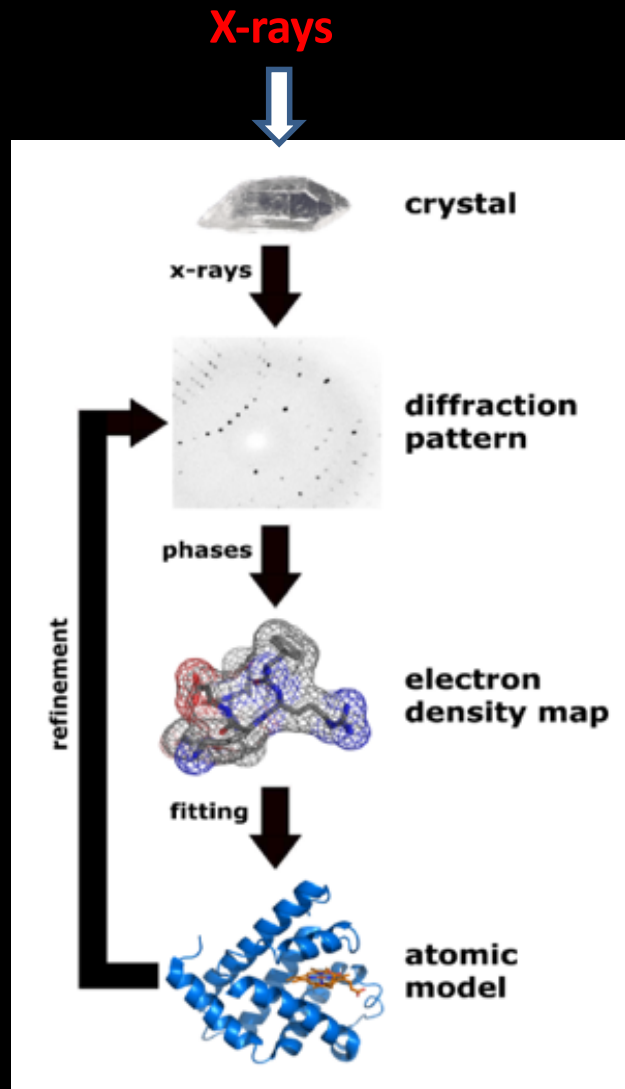
SensL (<http://sensl.com/>)

20x20 μm^2 , 35x35 μm^2 , 50x50 μm^2 , 100x100 μm^2 pixel size



Applications: Protein crystallography

Cinzia Da Via, Uni. Manchester IEEE NPSS Workshop on Applications of Radiation Instrumentation, 2020

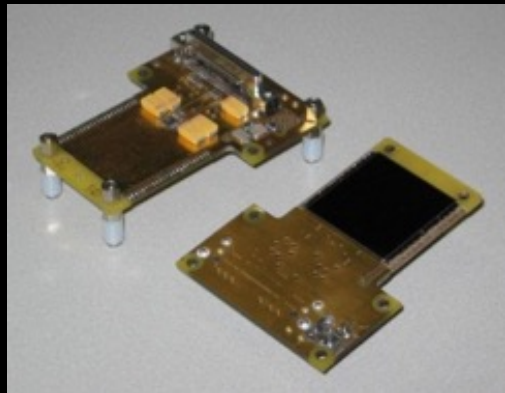


X-ray diffracted Photographic image of the double helix taken in 1952 by Rosalind Franklin and Raymond Gosling. The DNA sample was fibrous DNA

Some of the existing electronics chips

Cinzia Da Via, Uni. Manchester IEEE NPSS Workshop on Applications of Radiation Instrumentation, 2020

Single photon Counting



Medipix2 Quad
 Pixels: 512 x 512
 Pixel size: 55 x 55 mm²
 Area: 3 x 3 cm²

Mithen II



Eiger



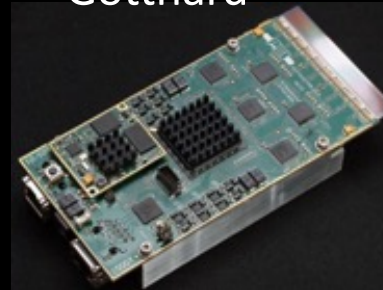
Medipix

pixellated detector
 (Si, GaAs, CdTe, 3D
 thickness:
 300/700/1000mm

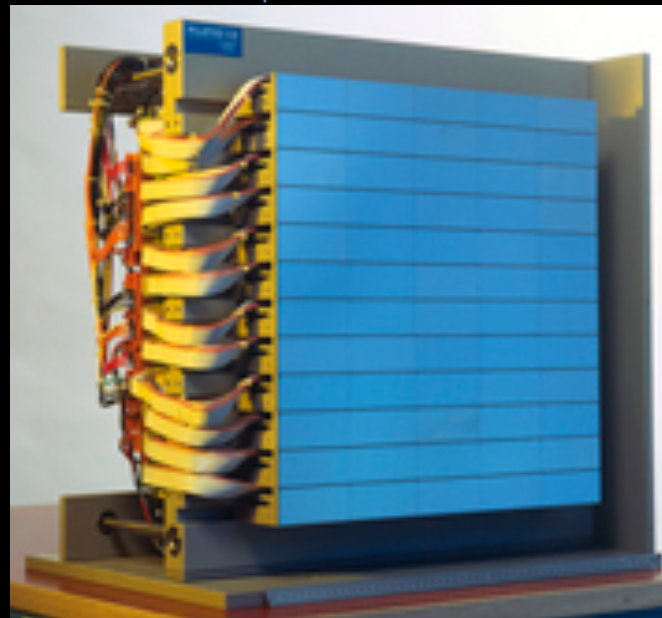
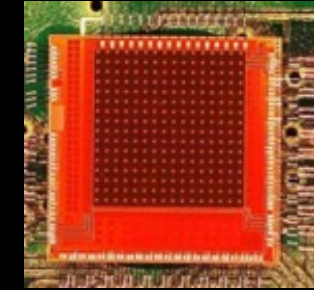
MORE ON THIS!

Charge Integration

Gotthard



AGIPD



The PILATUS 6M,

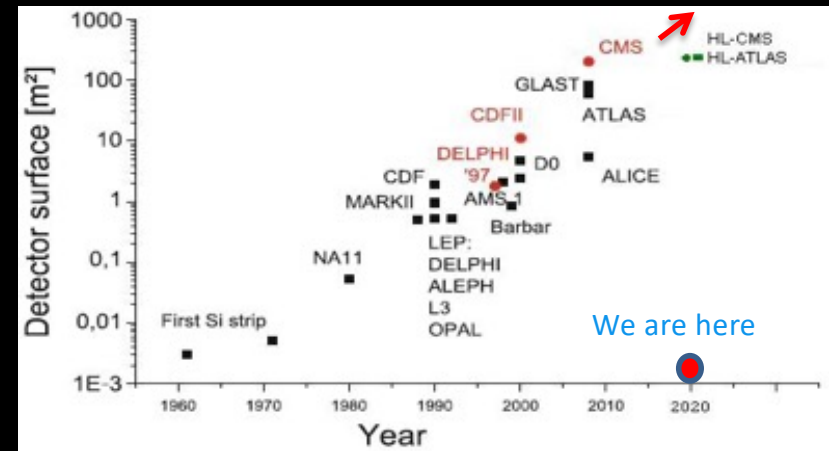
424 x 435 mm² with 170
 × 170 μm² (2463 x 2527)
 6 million pixels, has been
 developed at PSI and
 commercialized by the
 company Dectris for
 synchrotron imaging

Conclusions and Reflections

We had a look at some properties and parameters of strips and pixel detectors and their evolution since their first use in scientific applications (a lot is missing..)

I would encourage you to meditate on:

- ❖ How the signal is formed and detected
- ❖ How a detector design develops depending on applications and constraints
- ❖ On the past ideas looking towards the future challenges
- ❖ On the new ideas (including your own) which might look crazy now but might reveal a true innovation in few years time
- ❖ Don't be scared to be different!!!!



Books on silicon detectors

- Rossi, Fisher, Rohe and Wermes. Pixel Detectors from fundamentals to applications. Springer
- Helmut Spieler. Semiconductor detector systems. OUP Oxford
- Gerard Lutz. Semiconductor Radiation Detectors. Springer
- W. R. Leo. Techniques for Nuclear and Particle Physics Experiments. Springer-Verlag
- C. DaVia, GF. Dalla Betta, S. Parker, Radiation Sensors with 3D electrodes, CRC Press

Thanks to:

Daniela Bortoletto, CERN Summer Student Lectures
Patrick Le Du, EDIT School
Helmut Spieler, Lecture notes (IBL)
Hartmut Sadrozinski, GianLuigi Casse,
Michael Moll, PhD Thesis
Steve Watts, CERN Academic Training
Harris Kagan,
Roland Horisberger,
Marco Povoli, PhD thesis
Gregor Kramberger
Andrea Castoldi,
Chris Damerell,
Sherwood Parker,
Erik Heijne,
Ariella Cattai
Giulio Pellegrini
GianFranco Dalla Betta
Adriano Lai